공학박사학위논문

Polymerization and Physical Properties of Benzoxazine Based Thermosetting Resin and Thermotropic Liquid Crystalline Polyester

벤조옥사진 열경화 수지와 열방성 액정 폴리에스터의 중합 및 물성 연구

2018 년 2 월

서울대학교 대학원

재료공학부

이 선 호

Polymerization and Physical Properties of Benzoxazine Based Thermosetting Resin and Thermotropic Liquid Crystalline Polyester

벤조옥사진 열경화 수지와
열방성 액정 폴리에스터의 중합 및 물성 연구

지도교수 안 철 희

이 논문을 공학박사학위논문으로 제출함
2017 년 12 월

서울대학교 대학원
재료공학부
이 선 호

이 선 호 의 공학박사학위논문을 인준함
2017 년 12 월

위 원 장 유 웅 열 (인)
부위원장 안 철 희 (인)
위 원 김 종 량 (인)
위 원 김 미 영 (인)
위 원 홍 성 우 (인)

Abstract

Polymerization and Physical Properties of Benzoxazine Based Thermosetting Resin and Thermotropic Liquid Crystalline Polyester

Seon Ho Lee

Department of Materials Science and Engineering

College of Engineering

Seoul National University

Epoxy resin has been known as a good candidate for a printed circuit boards (PCBs) material since its excellent mechanical strength and adhesion property to metal. Polybenzoxazine, a thermosetting polymer and strong candidate as an industrially applicable material, has attracted attentions recent years as a novel electrical insulating material displaying excellent thermal stability. Benzoxazine and epoxy/silica nanoparticles were

employed to prepare thin film exhibiting ultra-low dissipation factor. In Chapter 2, two types of thermosetting benzoxazine precursors, monobenzoxazine and linear polybenzoxazine, were synthesized in bulk or solution condition, respectively. For monobenzoxazine/silica hybrid film, the epoxy was additionally used to improve its physical stability. With different wt % composition of monobenzoxazine/epoxy, a higher content of monobenzoxazine showed reduced dissipation factor (~ 0.005 frequency/10 GHz) with lower mechanical stability. On the contrary, linear polybenzoxazine/silica hybrid film demonstrated dramatically enhanced mechanical stability possibly due to its higher molecular weight network structure. However, due to its lack of polar functional group, it showed less adhesion ability to copper layer. To overcome these drawbacks, linear polybenzoxazine and epoxy blend system was prepared to increase adhesion to the copper foil and electrical insulation property (dissipation factor = ~ 0.006). In chapter 3, benzoxazine containing cyano group was synthesized. The cyano group in cyano-benzoxazine forms a triazine ring through the thermosetting process. The triazine ring increases the insulating property by diluting dipole concentration and electronegativity. In this study, silica hybrid films were prepared by the thermosetting process using highly insulating cyano-benzoxazine. Since the film obtained through the thermal

curing process of cyano-benzoxazine showed brittle properties, epoxy resin was added to enhance the mechanical properties. As the content of cyano-benzoxazine increased, a lower dissipation factor was observed (dissipation factor = ~ 0.004).

The thermotropic liquid crystalline polymers represent an anisotropic molten state above the melting point of the polymer. Thermotropic liquid crystalline have high mechanical strength and excellent resistance against heat and chemical. Due to these characteristics, thermotropic liquid crystals are widely used in various industries where electrical components or high mechanical properties are required. Ekonol, which is most common form of thermotropic liquid crystalline polyester (TLCP), requires high temperature for processing due to its high melting point. In order to decrease the melting point of TLCPs, the introduction of non-linear monomers, aliphatic monomers and lateral substituents have been proposed. In chapter 4, several compositions of *p*-HBA, 6-Hydroxy-2-naphthoic acid (HNA), resorcinol, 4,4'-biphenol (BP) and terephthalic acid (TPA) were copolymerized to control melting point and provide optimized mechanical properties. Higher content of resorcinol and HNA in the polymerization of TLCP yield lower melting point which provide enhanced

processibility.

Keywords : Benzoxazine, epoxy, silica, hybrid film, dissipation factor, liquid crystalline polyester, melting point

Student Number **:** 2010-23194

Contents

Chapter 4.

List of Tables and Schemes

List of Figures

Chapter 1.

Introduction

1.1. Application and classification of PCBs

Printed circuit boards (PCBs), patterned with electric circuit on an insulating plate, are the substrates to connect and support electronic components and semiconductors [1]. PCBs are the most basic electrical components used in household appliances, automobiles and advanced electrical products. PCB have many advantages such as wide range of application, high stability and easy manufacturing. Depending on the application of the electronic product, shape of PCBs can be modified. Easy manufacturing enables mass production with reliable production quality. For these reasons, PCB can contribute to the miniaturization of electronics without sacrifice stability

The material of the PCBs is required to have properties such as insulation resistance, chemical resistance, heat resistance, workability and appropriate mechanical strength. These properties of the PCBs depend on the characteristics of the polymer resins. PCBs can be classified as single-side PCB, double-side PCB, multi-layer PCB and flexible PCB according to their number of wiring circuit layers. Single-side PCB is mainly used for products with relatively simple circuit configuration such as radio or telephone. Double-side PCB and multi-layer PCB are used in electrical

products that perform complex instructions such as TV and computer. Flexible PCBs [2] are used in the fields such as flexible display.

1.2. Research Status for Insulating Multi-layer PCBs

As the use of multi-layer substrates increases with the miniaturization of electronic devices, it is important to make the insulation layer ultra-thin for high-integration of circuits. Even though the thickness of the interlayer in the PCB is very thin, there is a demand for materials having excellent insulating property, heat resistance and mechanical strength. In addition, due to the development of telecommunication equipment, the high frequency and the high speed of the signal applied to the PCB which cause problems such as transmission loss and signal delay [3]. Therefore, materials that lowering transmission loss and signal delay are also in demand. Since the transmission loss is mostly affected by the dissipation factor, signal delay is increased as dissipation factor increases. For this reason, the dielectric polarization in the substrate material must be minimized in order to produce electrically insulating materials. Epoxy resins [4], [5], the most commercially available thermoset material, have been widely used in the field of PCBs with their various advantages such as inexpensive price,

simple to control molecular structure, excellent in mechanical properties, and easy to develop composite materials with inorganic materials. However, the hydroxyl groups, which are generated in the thermosetting process, cause a negative effect on dissipation factor, which is an evaluation index of electrical insulation. With the development of electronic devices that experience high frequencies, dissipation factor is becoming more important in the insulation evaluation index.

Polymeric resins have been studied to develop insulating materials with lower dissipation factor to replace the epoxy resin. Polycyanate [6], [7] and polydicyclopentadiene [8] are the polymeric resins that show excellent electrical insulating. However, they show brittle nature and low adhesion to the copper foil. To overcome those drawbacks, studies have been actively conducted to increase the insulation and mechanical strength through the development of hybrid materials by introducing inorganic materials such as silica nanoparticles into organic materials [9], [10]. Bezoxazine, epoxy and cyanate esters are examples of the organic materials and their structures and properties are shown in Table 1-1.

1.3. Research Objectives (PCB)

Benzoxazines are industrially important thermosetting polymer resins in terms of excellent electrical insulating property and heat resistance. Benzoxazines are synthesized using various types of phenols and primary amines [11], which show excellent potential for chemical structural modification. Benzoxazines are simply synthesized under bulk or solution conditions with a short time and they are polymerized through a thermosetting process without any catalyst [12], [13], and there is no byproduct like volatile gas in this process. The hydroxyl groups-generated through the thermal curing process are tied up by inter- and intramolecular hydrogen bonding [14], so that the benzoxazines have an effect of inhibiting the dielectric polarization which is caused by the external electromagnetic field. For this reason, benzoxazines are classified as a thermosetting resin with excellent insulating property [15], [16], [17]. In the past research, the typical thermosetting temperature of benzoxazine has been reported to be over 200 ^{o}C. Therefore, a large energy cost is required for the process of fabricating the insulating material.

In chapter 2, development of benzoxazine-based silica particle hybrid benzoxazine mixture was carried out at a temperature not exceeding 200 ^{o}C, and then DSC (differential scanning calorimeter) analysis confirmed

completion of curing. Hybrid films produced under these thermosetting

Table 1-1. Candidate of thermosetting polymer

Thermosetting polymer	Property
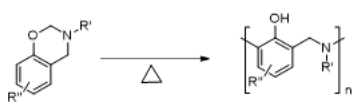 **Benzoxazine**	• **Electric insulation property** • Non production of volatile gas during combustion • Easy to control molecular structure
 **Epoxy**	• **Strong adhesion to copper foil** • **Mechanical flexibility** • Easy to control molecular structure
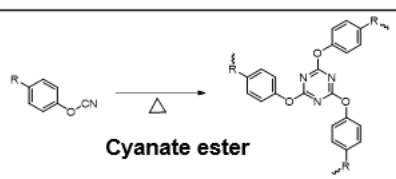 **Cyanate ester**	• **Electric insulation property** • Brittleness nature of produced film

condition exhibited reduction of dissipation factor compared to conventional epoxy-based hybrid films. The benzoxazines used in this study were monobenzoxazines and linear polybenzoxazine. Since the monobenzoxazine/silica hybrid film without epoxy was brittle, epoxy resin was added to increase the mechanical strength for the production of PCB materials. The reduction of dissipation factor with increasing monobenzoxazine content was achieved, but the mechanical strength was still weak. In order to improve this limitation, linear polybenzoxazine was used instead of monobenzoxazine and stable mechanical strength was achieved even though no epoxy was added. However, the hydroxyl groups formed in the thermal curing process of linear polybenzoxazine were not adhered to the copper foil due to inter- and intramolecular hydrogen bonding between the polymers. Therefore, the epoxy resin was introduced to linear polybenzoxazine/silica hybrid film to overcome this problem. As a result, reduced dissipation factor with excellent adhesion to copper foil were achieved. Figure 1-1 shows the concept of this experiment.

In chapter 3, benzoxazine containing cyano group was synthesized. Epoxy and silica nanoparticles were introduced into the hybrid films. Cyano

group in cyano-benzoxazine participate in the thermosetting reaction forming

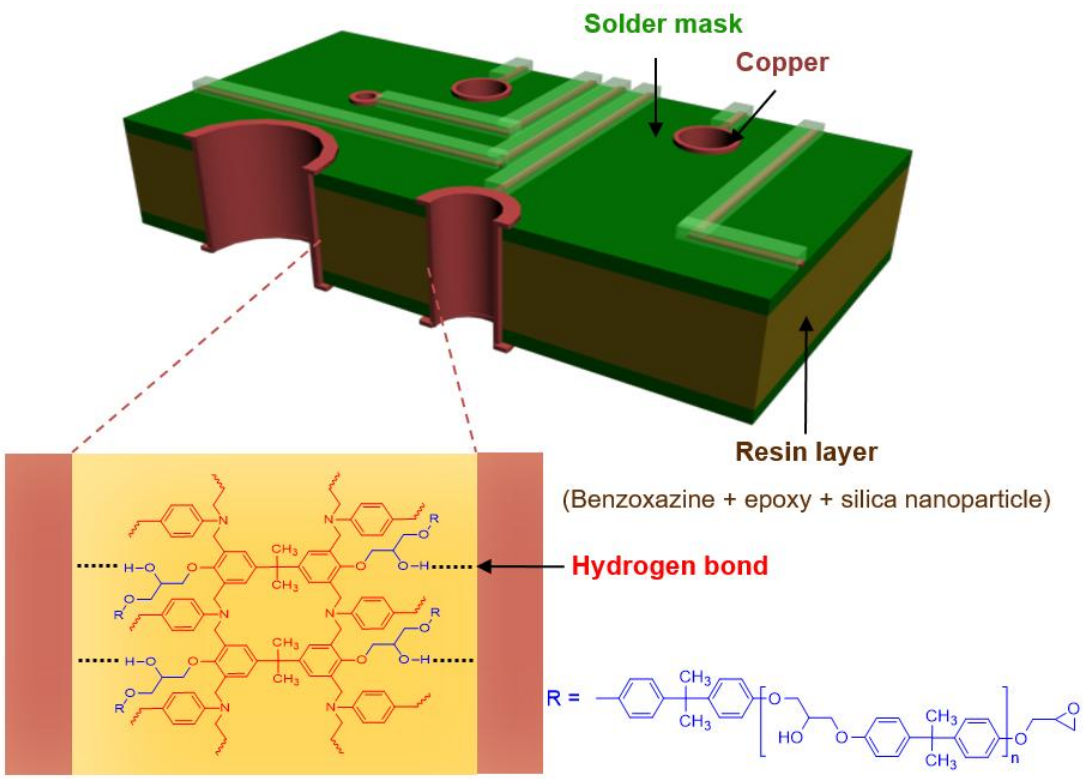

Figure 1-1. Experimental concept of PCB materials

triazine ring. In general, as a bulkiness of hydrocarbons increases, the electronegativity decreases and the dipole concentration is diluted resulting improvement of the insulation property. The triazine formed in the thermal curing process of cyano group is reported as an excellent electrical insulation group with their bulkiness. Although the cyano group has a disadvantage of high temperature condition of 200 ^{o}C or more, cyano-benzoxazine-based hybrid film showed a reduced dissipation factor compare to normal monobenzoxazine-based hybrid film.

1.4. Types and classification of liquid crystals

A liquid crystal is a material having a regular arrangement with fluidity characteristic of a liquid. This material is widely used in the field of the display because changes in the molecular arrangement under voltage or temperature are optically visible. Liquid crystals are classified as thermotropic and lyotropic [18], [19]. The thermotropic liquid crystal maintains anisotropic melting state at a temperature above the melting point, and the lyotropic liquid crystal exhibits anisotropic properties when dissolved in a solvent above a critical concentration. The most typical example of a lyotropic liquid crystal is an amphipathic molecule such as a surfactant, which is specifically oriented in a solvent to form a liquid crystalline phase. According to liquid crystal phase, liquid crystal can be classified as nematic, smectic and cholesteric. The nematic liquid crystals have an irregular molecular position but have a directional arrangement only because the molecules are oriented in a uniform direction. This material exhibits elastic properties since it is relatively low ~~in~~ viscosity and easily deformed by

external forces. The smectic liquid crystals have not only a direction but also a position order because the molecules are arranged in a uniform direction, thus the molecules themselves form a layer. The smectic phases are classified into smectic-A, smectic-B, smectic-C, smectic-E, smectic-F and smectic-G depending on the angle between the long axis of the molecule and the fault plane. The cholesteric liquid crystals have a structure in which the nematic layer rotates at a certain angle. Cholesterol is one example of molecules that form this phase.

1.5. Physical properties according to chemical structure of liquid crystalline polymers

Liquid crystals are divided into monomer and polymer types according to molecular weight. Unlike general crystalline polymers, liquid crystalline polymers have a high degree of orientation with a specific direction in a molten state for the reason that they are mainly rigid aromatic structure. Liquid crystalline polymers are the high-performance fiber with 5 times better elasticity and strength than steel, therefore they are widely used as structural materials [20] such as body armor, tire cords, electrical products and advanced materials. Also, liquid crystalline polymers are mainly applied

in the field where high temperature and high load condition are constantly introduced because of its excellent heat resistance. Due to these properties, liquid crystalline polymers are suitable for the structural materials that can be used under high temperature and constant load.

The major chemical bond of the liquid crystalline polymer structure is ester or amide. Among these liquid crystalline polymers, commercialized structure with an amide bond is Kevlar [21], [22], which is polymerized in a *p*-position aromatic structure to form intermolecular hydrogen bonding. Because of its chemical structure, Kevlar has excellent physical properties and is used as a constituent material of the body armor. However, there is a limitation in processibility due to high melting point and low solubility in solvent. Eknol [23], [24] and Vectra A are commercialized liquid crystalline polymer that polymerized with ester bond. Ekonol is a homopolymer of *p*-hydroxybenzoic acid (*p*-HBA) and has a melting point of over 500 ^{o}C, which limits its processing. Vectra A is a polymer composed of *p*-HBA and 6-hydroxy-2-naphthoic acid (HNA) and has a relatively good processibility with a melting point of about 280 ^{o}C. Because of the structural property of HNA, the crankshaft effect appears, which leads to a decrease in melting point. Due to excellent processibility and miscibility with other polymers,

blend studies are actively performed [25], [26].

To make an easy processible liquid crystalline polymer, additional unit is required for lowering melting point along with mesogenic unit for liquid crystallinity property. Based on Ekonol, various types of thermotropic liquid crystalline polyesters (TLCPs) have been studied through chemical structural changes. In order to lower the melting point, flexible aliphatic spacers, units with substituents, units with *m*-position, and kink units are introduced into the backbone [27], [28], [29], [30], [31]. As a result of introducing these units, the π-π stacking of the aromatic polymer is inhibited, thereby lower the melting point. Depending on the amount of the added units, the melting point of the polymerized TLCPs are changed, which makes it possible to design TLCPs suitable for various application site. Figure 1-2 shows examples of processible TLCPs.

1.6. Characterization methods of TLCP

In order to confirm whether the polymer forms liquid crystallinity, various analytical methods are developed such as a polarizing microscope, differential scanning calorimetry (DSC) and X-ray scattering.

One of the important characteristics of the TLCPs is the anisotropic state in the molten state, which can be confirmed by using a polarizing microscope. Similarly, DSC analysis is another method of confirming liquid

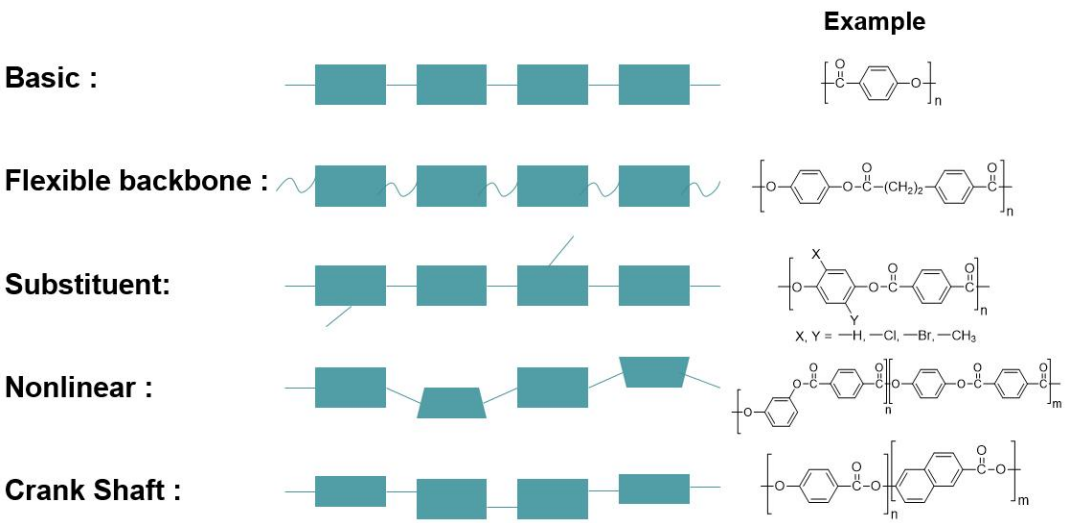

Figure 1-2. Structure for processible TCLPs

crystallinity. In the DSC analysis process, as the TLCP melts, the chains of the crystalline portion are released and an endothermic peak is generated. When the temperature further increases, an isotropic transition peak appears. This peak tendency is different from crystalline polymers such as polyethylene terephthalate (PET). The other method of liquid crystallinity analysis is through X-ray scattering. The intensity and diffraction angle of the light can be analyzed through this method. In the case of TLCPs, crystallinity is maintained before and after melting point. On the other hand, the crystalline polymer, PET, has a large change in X-ray diffraction pattern after melting point.

1.7. Research Objectives (TLCP)

Among the commercialized TLCPs, Vectra A is obtained by polymerizing *p*-HBA and HNA in a mol ratio of 73:27. Vectra A has melting point about 280 ^{o}C [32]. Polymerization studies are actively investigated with a large number of different monomers to replace HNA. Monomer candidates

are *m*-HBA, resorcinol, and isophthalic acid (IPA).

In Chapter 4, a commercially available TLCP study was conducted. In this experiment, we set the melting point and physical property of Vectra A as a target objective. Resorcinol, which is a strong candidate to increase TLCP processibility, was added to replace the HNA of the added monomers because HNA is a relatively expensive monomer. Resorcinol has two hydroxyl groups at *m*-position, so they are able to substitute for HNA. The polymerization method was carried out by a condensation polymerization. First, the hydroxyl groups of the monomers were activated by acetylation using acetic anhydride. Finally, the monomers were reacted with each other by decompression at high temperature to obtain the high-molecular-weight of TLCP. The mechanical properties of the obtained polymer were compared with Vectra A and the possibility of commercialization was confirmed.

1.8. References

[1] J. Li, H. Duan, S. Wang, *J. Air & Waste Manage. Assoc.* **2010**, *60*, 229.

[2] A. C. Siegel, S. T. Phillips, M. D. Dickey, N. Lu, Z. Suo, G. M. Whitesides, *Adv. Funct. Mater.* **2010**, *20*, 28.

[3] J.-Y. Shieh, H.-J. Hwang, S.-P. Yang, C.-S. Wang, *Journal of Polymer Science: Part A: Polymer Chemistry* **2005**, *43*, 671.

[4] M. Lé-Magda, E. Dargent, J. A. S. Puente, A. Guillet, E. Font, J.-M. Saiter, *Journal of Applied Polymer Science* **2013**, *130*, 786.

[5] K. Kadotani, *Composites* **1980**, *11*, 199.

[6] D. Mathew, C. P. R. Nair, K. Krishnan, K. N. Ninan, *Journal of Polymer Science: Part A: Polymer Chemistry* **1999**, *37*, 1103.

[7] H.-J. Hwang, C.-H. Li, C.-S. Wang, *Polymer* **2006**, *47*, 1291.

[8] J. H. Wang, G. Z. Liang, H. X. Yan, S. B. He, *eXPRESS Polymer Letters* **2008**, *2*, 118.

[9] J.-J. Park, *Trans. Electr. Electron. Mater.* **2012**, *13*, 322.

[10] C. Yan, X. Fan, J. Li, S. Z. Shen, *Journal of Applied Polymer Science* **2011**, *120*, 1525.

[11] X. Ning, H. Ishida, *Journal of Polymer Science: Part A: Polymer Chemistry* **1994**, *32*, 1121.

[12] H. Ishida, Y. Rodriguez, *Polymer* **1995**, *36*, 3151.

[13] T. Takeichi, T. Kano, T. Agag, *Polymer* **2005**, *46*, 12172.

[14] H.-D. Kim, H. Ishida, *J. Phys. Chem. A*. **2002**, *106*, 3271.

[15] Y.-C. Su, F.-C. Chang, *Polymer* **2003**, *44*, 7989.

[16] Y. Wang, K. Lou, Z. Li, G. Wu, Y. Zhang, A. Feng, *High Performance Polymers* **2016**, *28*, 1235.

[17] K. Zhang, Q. Zhuang, Y. Zhou, X. Liu, G. Yang, Z. Han, *Journal of Polymer Science: Part A: Polymer Chemistry* **2012**, *50*, 5115.

[18] J. Kotz, S. Kosmella, *Current Opinion in Colloid & Interface Science* **1999**, *4*, 348.

[19] M. A. DePierro, C. A. Guymon, *Macromolecules* **2014**, *47*, 5728.

[20] D. J. Williams, *Advances in Polymer Technology* **1990**, *10*, 173.

[21] T. I. Bair, P. W. Morgan, F. L. Killian, *Macromolecules* **1977**, *10*, 1396.

[22] M. Zhou, V. Frydman, L. Frydman, *J. Phys. Chem.* **1996**, *100*, 19280.

[23] H. R. Kricheldorf, G. Schwarz, *Makromol. Chem.* **1983**, *4*, 475.

[24] J. Economy, R. S. Storm, V. I. Matkovich, S. G. Cottis, B. E. Nowak, *Journal of Polymer Science: Part A: Polymer Chemistry* **1976**, *14*, 2207.

[25] T.-T. Hsieh, C. Tiu, K.-H. Hsieh, G. P. Simon, *Korea-Australia Rheology Journal* **1999**, *11*, 255.

[26] P. Tang, J. A. Reimer, M. M. Denn, *Macromolecules* **1993**, *26*, 4269.

[27] W. J. Jackson, *Polymer International* **1980**, *12*, 154.

[28] Z. Yerlikaya. S. Aksoy, E. Bayramli, *Journal of Polymer Science* **2003**, *90*, 3260.

[29] Z. Yerlikaya, S. Aksoy, E. Bayramli, *Journal of Polymer Science* **2002**, *85*, 2580.

[30] N. Khan, Z. Bashir, D. M. Price, *Journal of Applied Polymer Science* **1995**, *58*, 1509.

[31] D. Dong, S. Jiang, Y. Ni, B. Jiang, *European Polymer Journal* **2001**, *37*, 611.

[32] M. Koike, C.-C Yen, L. Yuqing, H. Tsuchiya, M. Tokita, S. Kawauchi, H. Takezoe, J. Watanabe, *Macromolecules* **2007**, *40*, 2524.

Chapter 2.

Development of Insulating Hybrid Materials Based on Monobenzoxazine and Linear Polybenzoxazine

2.1. Introduction

Printed circuit boards (PCBs) need to have functions of heat resistance and mechanical strength. A lot of approaches have employed thermosetting polymers as a candidate material.

Epoxy resins are most commonly used due to their commercial benefit and strong physical strength [1]. However single epoxy resin is difficult to be used as an electrical insulator with required insulating property due to the influence of free hydroxyl groups which are generated during thermal polymerization. To reduce dissipation factor, researches using thermosetting polymer including polycyanurate and dicyclopentadiene were reported [2], [3], [4], [5]. Hybrid materials consisting of thermosetting resin/silica were also reported for the enhanced electric insulating property at high-frequency, improved mechanical toughness and excellent thermal resistance [6], [7].

Since the first synthesis by Holly and Cope [8], benzoxazines are industrially important thermosetting polymer resins in terms of excellent electrical insulating property and heat resistance [9]. In addition, the formation of strong hydrogen bonding between hydroxyl and tertiary amine groups after ring-opening makes polybenzoxazine exhibit low water absorption and high T_g for good thermal stability [10]. Benzoxazines have been developed as a new series of phenolic resin and displayed the great potential with various molecular structures due to a large number of commercially available monomers containing phenols and primary amines. By Mannich reaction, benzoxazines are synthesized in a relatively simple way using hydroxyl-, amine-functionalized monomers and paraformaldehyde in bulk or solution condition. Benzoxazine ring formation is usually completed in a short reaction time [11]. Polymerization of benzoxazines is carried out by thermal treatment with the catalyst-free condition and polybenzoxazine is obtained without noticeable byproduct.

Films prepared from monobenzoxazines show limitation in mechanical properties due to inherent brittle nature [12], [13]. Several methods have been developed to endow the brittle films with toughness. One approach is a blend system with the other polymers such as epoxy or

polyurethane [14], [15], displaying better film-forming properties. Another method is to employ high-molecular-weight polybenzoxazine precursor which can be prepared by condensation polymerization of dihydroxyl and diamine-based monomers [16]. In addition to the enhanced toughness compared to normal monobenzoxazine-based film, different structures of difunctionalized monomers made it possible to prepare thermally cured linear polybenzoxazine-based films.

Herein, benzoxazine-based PCB hybrid materials for improved electrical insulation and mechanical properties were developed as shown Figure 2-1. Brittle nature of monobenzoxazine-based film required blend system with epoxy resin to meet the mechanical properties of a PCB film. Prepared hybrid films based on monobenzoxazines and epoxy exhibited a lower dissipation factor and improved physical strength. In case of linear polybenzoxazine and silica hybrid films, low dissipation factor was achieved along with excellent mechanical properties without epoxy resin. However, phenol groups in single benzoxazine system did not provide sufficient adhesion to copper. Therefore, linear polybenzoxazine/silica hybrid film also required blend system with epoxy resin. Finally, optimized blend composition of the hybrid films was experimentally selected to

prepare a film displaying enhanced mechanical strength, copper adhesion and low dissipation factor. The chemical structures of benzoxazines and epoxy, thermosetting resins used for the production of hybrid films in this study, are displayed in Scheme 2-1.

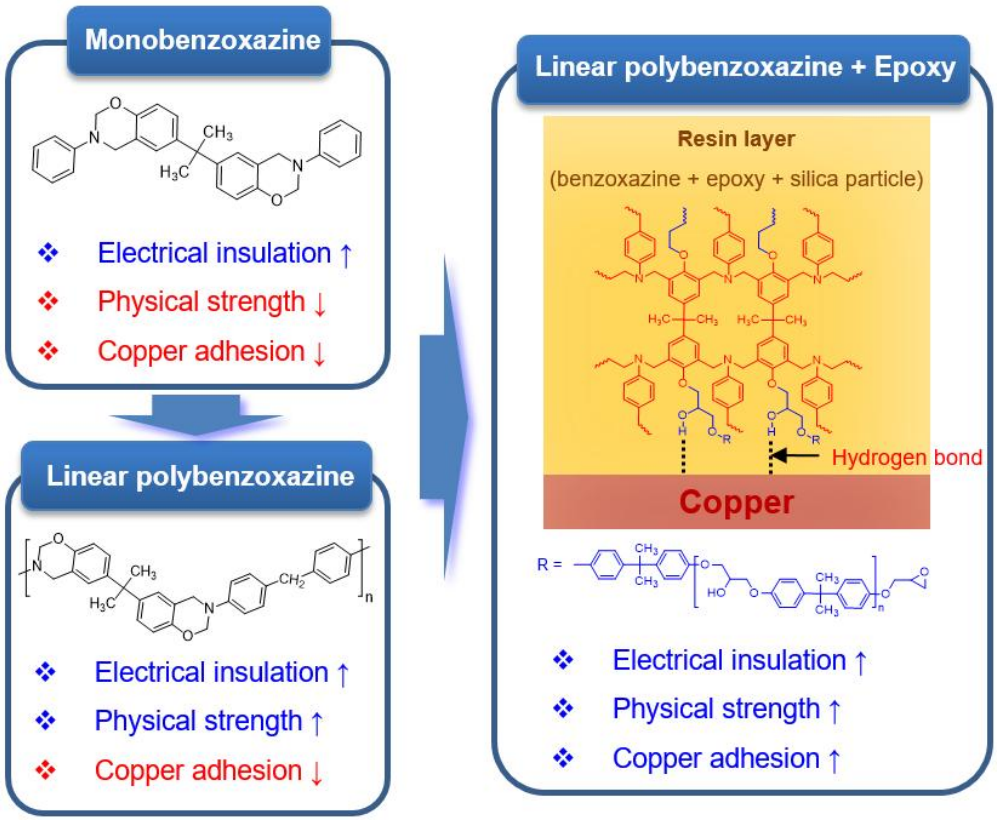

Figure 2-1. Experimental concept of PCB film

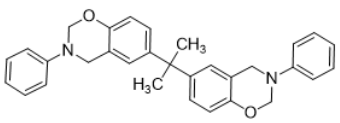

Monobenzoxazine (BA-a)

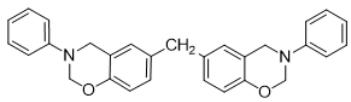

Monobenzoxazine (BF-a)

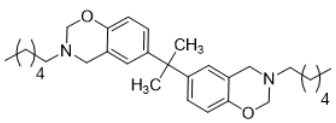

Monobenzoxazine (Hexyl-benzoxazine)

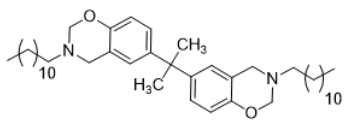

Monobenzoxazine (Dodecyl-benzoxazine)

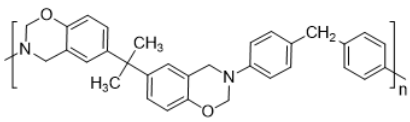

Linear polybenzoxazine

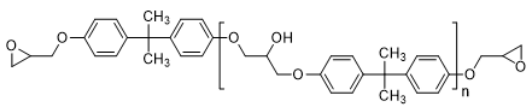

Epoxy (YD-128)

Scheme 2-1. The chemical structure of thermosetting resins

2.2. Experimental

Materials. Bisphenol A (99 %), $NaHCO_3$ (99.5 %), 1,4-dioxane

(99.5 %) and chloroform (99.5 %) were obtained from Daejungchem. Hexylamine (99 %), dodecylamine(> 99 %), paraformaldehyde (95 %), 4,4'-diaminodiphenylmethane (97 %), 4-dimethylamino pyridine (DMAP, 99 %) and cyclohexanone (99 %) were purchased from Sigma-Aldrich. Monobenzoxazines (BA-a: bisphenol A-based benzoxazine, BF-a: bisphenol F-based benzoxazine) were kindly supplied by Huntsman. Epoxy with the trade name of YD-128 (epoxy equivalent weight, EEW: 184~190 g/eq) and phenoxy thermoplastic were obtained from Kukdo., Ltd. PS-6313 (equivalent weight: 148 g/eq), epoxy curing agent, was obtained from Gun Ei Chemical Industry., Ltd. Leveller, whose name is BYK 337, was received from BYK. Active-ester catalyst with the trade name of HPC-8000-65T (equivalent weight: 223 g/eq) was acquired by DIC., and silica nanoparticles slurry coated by epoxy was purchased from Admatechs.

Synthesis of Aliphatic Benzoxazine. To prepare hexylamine-based benzoxazine (Hexyl-benzoxazine), paraformaldehyde (2.9 g, 96.4 mmol) and hexylamine (5.2 g, 48.2 mmol) were placed in a two-neck round bottom flask equipped with a magnetic stirrer. After equipped in an oil bath heated to 95 ^{o}C, stirring was performed. After 10 min, bisphenol A (5.0 g, 21.8

mmol) was added to the reaction mixture and stirred for an additional 20 min. After completion of the reaction, the mixture was cooled to 50 ^{o}C and dissolved in 25 ml of chloroform. The solution was washed several times with 1 N NaOH and deionized water. Finally, the organic solution was dried with $MgSO_4$, filtered and dried in a 25 ^{o}C vacuum oven for 24 h. Dodecylamine-based benzoxazine (Dodecyl-benzoxazine) was also synthesized as described above. The synthetic method is shown in Scheme 2-2 (a).

Synthesis of linear polybenzoxazine. As displayed in Scheme 2-2 (b), linear polybenzoxazine was synthesized using the reported method [16]. 260 mL chloroform dissolving bisphenol A (20.0 g, 87.6 mmol), diaminodiphenylmethane (17.4 g, 87.6 mmol) and paraformaldehyde (10.5 g, 350.4 mmol) were charged to a 1 neck round-bottomed flask equipped with a reflux condenser. The mixture was refluxed with vigorous stirring for 5, 12, 36 and 72 h, respectively. After cooled to room temperature, the solution was filtered and washed with 1 N $NaHCO_3$, water and dried with magnesium sulfate. Finally, the organic layer was dropped into diethyl ether to take a

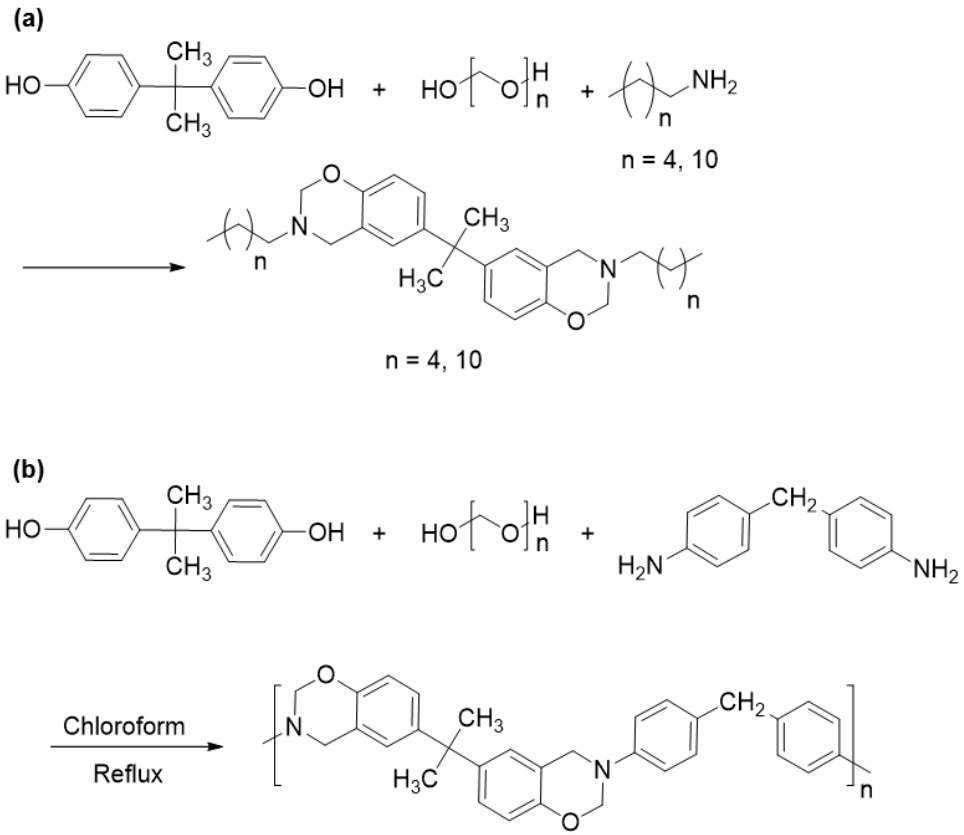

Scheme 2-2. Synthetic method of (a) monobenzoxazines and (b) linear polybenzoxazine

precipitated powder then filtered. The obtained powder was dried at 25 ^{o}C

in a vacuum oven for overnight.

Benzoxazine hybrid film. The monobenzoxazine structures BA-a, BF-a, Hexyl-benzoxazine and Dodecyl-benzoxazine-based films were all produced in the same way. As represented by monobenzoxazines, BA-a (2.00 g, 4.33 mmol) was dissolved in 6 mL 1,4-dioxane in a 70 mL vial. To the solution, phenoxy thermoplastic (0.57 g, 10.00 phr), leveller (0.24 g, 1.50 phr) and silica nanoparticles slurry (7.27 g, 70 wt % of the total reagent mixture) were added. After casting the mixture onto a copper foil with the size of 100 mm×100 mm×0.125 mm, solvent was evaporated at 80 ^{o}C for 10 min. After drying of the solvent, the film was cut into a size of 100 mm×3 mm×0.125 mm, then the curing process was performed. The film was sequentially cured at 180 ^{o}C for 2 h and 200 ^{o}C for 2 h. After curing, the copper foil was removed using 50 wt % nitric acid aqueous solution. The obtained hybrid film was rinsed with distilled water 3 times and dried at 90 ^{o}C for 3 h in an oven. Linear polybenzoxazine-based film was fabricated using the same method as described above.

Benzoxazine blend hybrid film. As represented by monobenzoxazines, BA-a (0.60 g, 1.30 mmol), epoxy (0.60 g), epoxy curing

agent (0.10 g, 11.68 phr), active-ester catalyst (0.76 g, 81.90 phr), phenoxy thermoplastic (0.50 g, 10.00 phr), DMAP (6.03 mg, 0.05 mmol), leveller (0.15 g, 1.50 phr) and epoxy functionalized silica nanoparticles slurry (6.40 g, 70 wt % of the total reagent mixture) were well mixed in 0.77 mL cyclohexanone in a 70 mL vial and cast on a copper foil with the size of 100 mm×100 mm×0.125 mm. Solvent drying was performed in the same method as described above, then the film was cut into a size of 100 mm×3 mm×0.125 mm. After curing, the work-up process followed the same method mentioned above.

Linear polybenzoxazine-based hybrid film was fabricated using 0.6 g polymer in 1.8 mL 1,4-dioxane solution. Weight ratios of the other reagents were the same as described above.

BA-a and polybenzoxazine hybrid films with a different weight ratio of benzoxazine and epoxy were prepared using the same method mentioned above. The amount of epoxy curing agent, active ester catalyst and DMAP were calculated proportional to the content of epoxy. The amount of phenoxy thermoplastic was calculated proportional to the contents of benzoxazine and the amount of epoxy blend, and silica nanoparticle slurry and leveller were calculated proportionally to the total

reagent mixture. The following abbreviation was coined: BA-a 1 stands for the blend composed of 1:1 weight ratio of BA-a: epoxy, and BA-a 2 for the 2:1 weight ratio of BA-a:epoxy. Linear polybenzoxazine 1 and 2 stand for the same weight ratio of the blend system.

Instruments. ^{1}H nuclear magnetic resonance (^{1}H NMR) were carried out on an Advance-300 (Bruker) with deuterium chloroform as a solvent at 300 MHz frequency. Gel permeation chromatography (GPC) was taken with CTO-10A (Shimadzu) at 40 ^{o}C using tetrahydrofuran as an eluent at the rate of 1.0 mL/min and the molecular weight was calculated with polystyrene standards. Differential scanning calorimetry (DSC) was performed with Q10 (TA instrument) at the heating rate of 10 ^{o}C/min under N_2 atmosphere. To proceed peel experiments, benzoxazine-based hybrid mixtures in solvent were cast on PET films and pre-cured at 80 ^{o}C for 10 min. A copper clad laminate (CCL) was placed on the pre-cured film, and lamination process was carried out to remove the PET film after compression at 90 ^{o}C for 60 sec with a pressure of 8 kgf/cm^2. After curing at 180 ^{o}C for 2 h and 200 ^{o}C for 2 h, desmear process was carried out on the film surface. A copper seed was introduced through an electroless plating process then a copper plating was conducted through an electroplating

process. Finally, the copper crystal growth was completed by heating at 170 ^{o}C for 1 h. The peel test was performed with the average surface roughness of 0.5 μm using copper clad laminate. The rate of crosshead movement was 10 mm/min and the analyzing temperature was 25 ^{o}C (10 mm×30 mm size) using universal testing machine (TA instrument). The dissipation factor was recorded with resonant cavity type microwave dielectrometer (AET, INC) on the frequency of 10 GHz at 25 ^{o}C. Before proceeding with the test, all the films (100 mm×3 mm×0.125 mm) were dried at 25 ^{o}C for 24 h in a vacuum oven.

2.3. Results and Discussion

Two different types of benzoxazines were employed in this study according to molecular weight: bisphenol A based monobenzoxazine and linear polybenzoxazine. One of the monobenzoxazine, Hexyl-benzoxazine was synthesized in 30 min under solvent-free conditions using bisphenol A, hexylamine and paraformaldehyde. After the reaction, it was dissolved in chloroform and washed several times with 1 N NaOH and water to obtain 85.4 % yield in pale yellow oil form. Dodecyl-benzoxazine was also synthesized in the same method as described above and was obtained with 88.1 % yield in yellow oil form. Linear polybenzoxazine was prepared with 1 mole of bisphenol A, 1 mole of diaminodiphenylmethane and 4 moles of paraformaldehyde in refluxing chloroform. The molar ratio of bisphenol A to diaminodiphenylmethane was precisely controlled to be an equimolar ratio in order to obtain a high-molecular-weight of linear polybenzoxazine. After pre-determined polymerization time at 5, 12, 36 and 72 h, the reaction mixture was washed with 1 N $NaHCO_3$ and water several times, then precipitated into diethyl ether to obtain white powder product. The higher-molecular-weight polymer was obtained with longer polymerization time and the isolation yield of linear polybenzoxazine obtained by reaction for 72

h was about 92 %. The polymerization results are summarized in Table 2-1. As prolonged reaction time, the higher-molecular-weight of linear polybenzoxazine was obtained. Preparation of linear polybenzoxazine-based film and measurement of the mechanical properties were performed using the polymers with the highest number average molecular weight of 9,300.

Several studies were reported that benzoxazine ring was not intact during the reaction at high temperature and closed-ring structures co-existed with the opened-ring structures in the reaction mixture [16], [17]. As shown in Figure 2-2 (a), Hexyl-benzoxazine was analyzed with the ^{1}H NMR spectrum. The presence of oxazine ring was confirmed by 4.9 and 4.0 ppm which respectively corresponds to -O-CH_2-N- and -Ar-CH_2-N-. From 6.6 to 7.2 ppm was assigned for aromatic protons. The methylene proton -N-CH_2-CH_2- was detected at 2.7 ppm. The methyl proton of -Ar-C(CH_3)$_2$-Ar- and methylene proton of CH_3-(CH_2)$_4$-CH_2- were marked at 1.5 ppm and 0.8 ~ 1.3 ppm, respectively. When the oxazine ring is completely closed, the theoretical proton ratio of oxazine and methyl group is 4:6. Thus, the ratio of the closed-ring structure was calculated as 95 %. Figure 2-2 (b) exhibits the ^{1}H NMR spectrum of Dodecyl-benzoxazine. The analysis method was same as above and the ratio of the closed-ring structure was 90%. Figure 2-3

shows a representative ^{1}H NMR spectrum of linear polybenzoxazine. The protons of

Table 2-1. Molecular weight of linear polybenzoxazines

Polymerization Time (h)	M_n	M_w / M_n
5	1,550	2.07
12	2,550	2.48
36	3,550	2.47
72	9,300	4.79

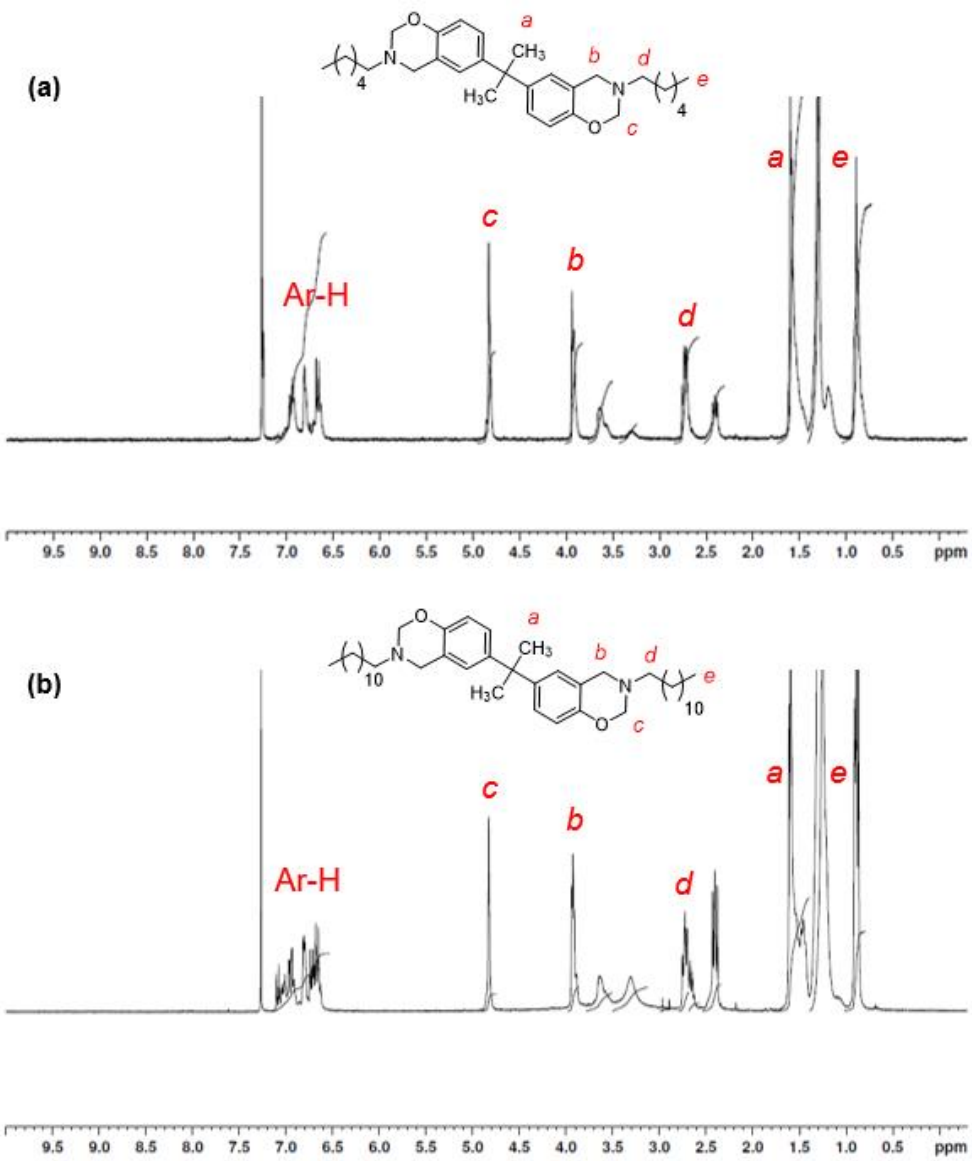

Figure 2-2. ^{1}H NMR spectra of (a) Hexyl-benzoxazine and (b) Dodecyl-benzoxazine

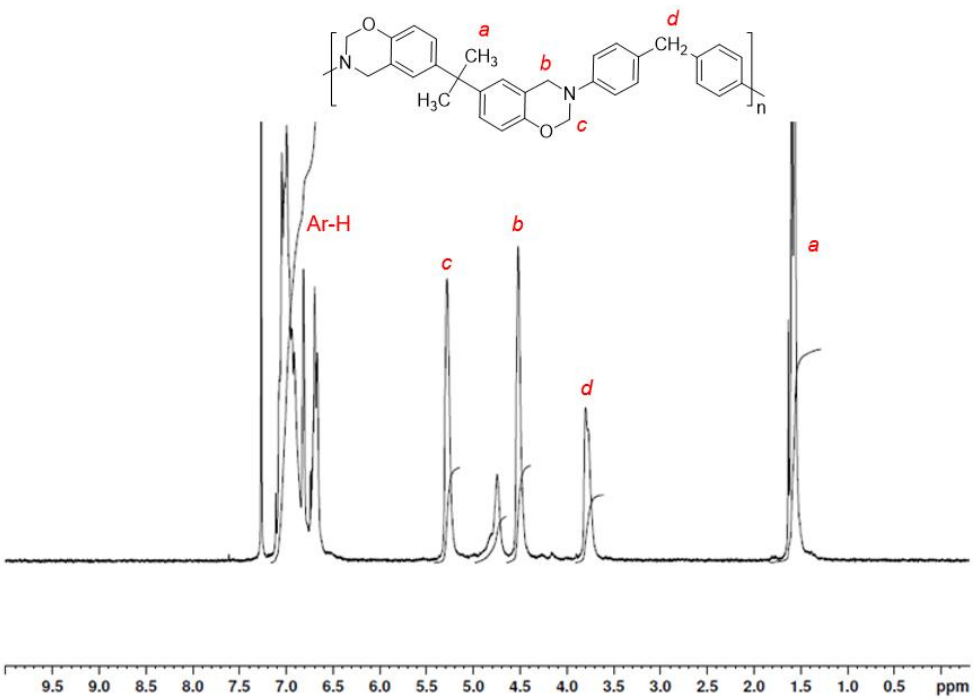

Figure 2-3. ^{1}H NMR spectrum of linear polybenzoxazine

oxazine ring appeared at 5.4 and 4.6 ppm, which respectively corresponds to -O-CH_2-N- and -Ar-CH_2-N-. The methyl proton of -Ar-C(CH_3)$_2$-Ar- and methylene proton of -Ar-CH_2-Ar- were detected at 1.5 and 3.8 ppm, respectively. The ratio of the closed-ring to intact oxazine rings was calculated to be 72 %. Considering previously reported ratio of 77 % [16], the increased percentage of opened-oxazine ring probably due to the prolonged polymerization time. A new peak from the opened-ring structure of benzoxazine ring was reported to appear around 3.8 ppm and it was difficult to separate the peak from that from methylene proton of bisphenol A. However, the obtained linear polybenzoxazine was clearly soluble in chloroform, THF and 1,4-dioxane at room temperature without any noticeable precipitates, which proved that the formation of network structure stemmed from ring-opening of oxazine was limited during the polymerization condition.

Previous researches have shown that exothermic curing peaks of benzoxazine generally appear at temperatures above 200 ^{o}C and that the curing process should proceed at higher temperatures [14]. Since a curing temperature below 200 ^{o}C was required in this study due to the device

conditions at Samsung Electro-Mechanics Co., optimized curing temperature was studied with the mixtures of benzoxazine and epoxy-coated silica nanoparticles.

Figure 2-4 shows DSC traces of neat monobenzoxazines and benzoxazine/silica nanoparticles (7/3 weight ratio) before and after sequential curing at 180 ^{o}C for 2 h and 200 ^{o}C for 2 h. The thermograms of neat BA-a with the heating rate of 10 ^{o}C/min displayed a curing exotherm at 228 ^{o}C. Similar to BA-a, exothermic peaks of BF-a, Hexyl-benzoxazine and Dodecyl-benzoxazine were measured at 235 ^{o}C, 236 ^{o}C and 214 ^{o}C, respectively. Even there were adjustments of chemical structural, no significant difference of exothermic peak and amount of exotherm was observed. Benzoxazine/silica nanoparticles mixtures, experienced the sequential curing conditions, were fully cured and the exotherm peaks completely disappeared, which led to a conclusion that the applied thermal conditions made a complete curing of the benzoxazine ring even at the temperature far below its peak temperature of curing exotherm. As shown in Figure 2-5, the change in exotherm enthalpy was confirmed by the thermal curing conditions of linear polybenzoxazine. Neat linear polybenzoxazine showed the exotherm peak at 160 ^{o}C. After the sequential curing with same

heat treatment as above method, the completion of the thermosetting was confirmed. From the results mentioned above, the

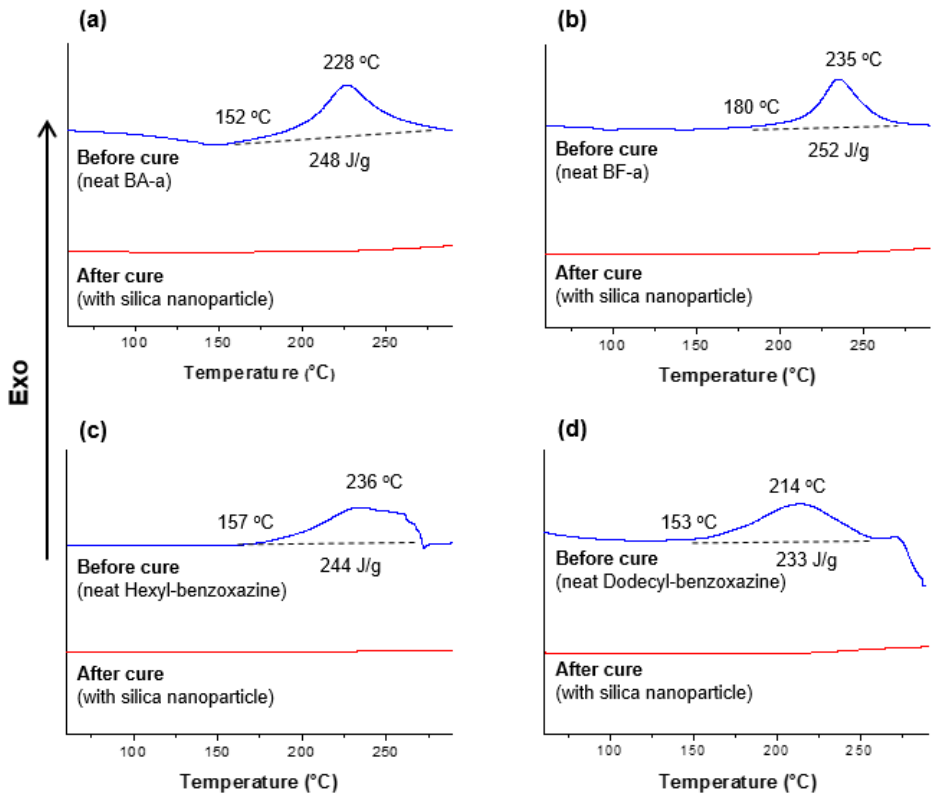

Figure 2-4. DSC trace of (a) BA-a, (b) BF-a, (c) Hexyl-benzoxazine and (d) Dodecyl-benzoxazine

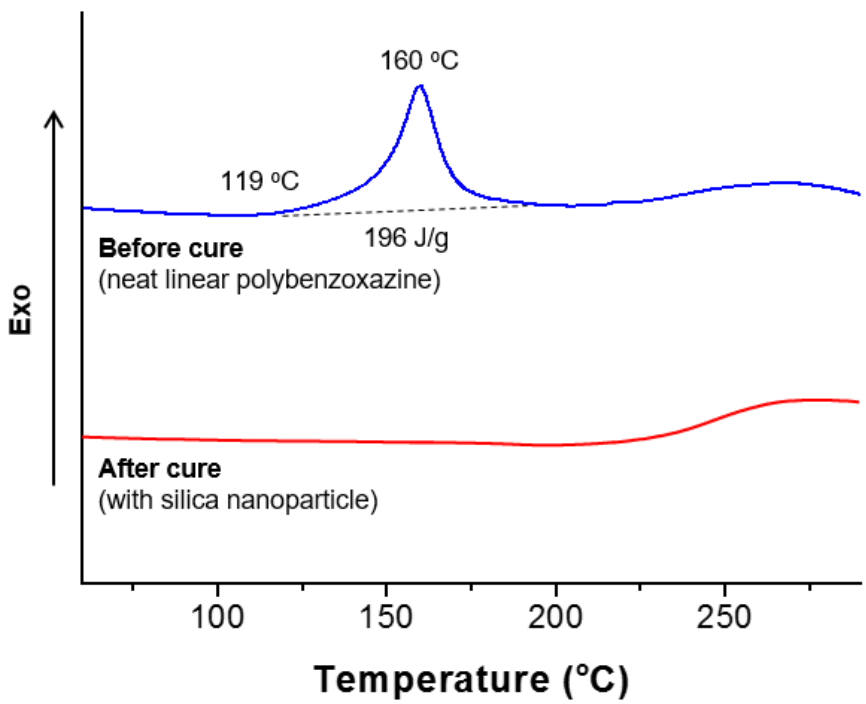

Figure 2-5. DSC trace of linear polybenzoxazine precursors

curing condition at 180 ^{o}C for 2 h and 200 ^{o}C for 2 h was set up in preparing for all the films in this study.

The films of benzoxazines and hybrids were prepared as described in the experimental section and the photos are displayed in Figure 2-6. As shown in Figure 2-6 (a), the film composed of BA-a and silica nanoparticles was so brittle that it was difficult to maintain a film but good enough to measure the dissipation factor with reliable reproducibility. As the amount of epoxy resin increased from BA-a 2 to BA-a 1, the prepared films exhibited improved mechanical properties. In case of linear polybenzoxazine, flexible films with the excellent mechanical property were fabricated and the film of neat linear polybenzoxazine showed the flexible property to be fully bent without any crack as exhibited in Figure 2-6 (d) and (e).

Generally, Epoxy resin is cross-linked with the presence of amine-based curing agents. If the same system is employed in the present study, non-reacted amine groups could produce a negative effect on dissipation

factor probably due to its highly polar nature. Therefore, it was investigated using isothermal DSC analysis whether the phenol groups generated during the curing of benzoxazine rings could play the role in curing epoxide rings. Figure 2-7 illustrates DSC traces of BA-a, epoxy and BA- a/epoxy blend with

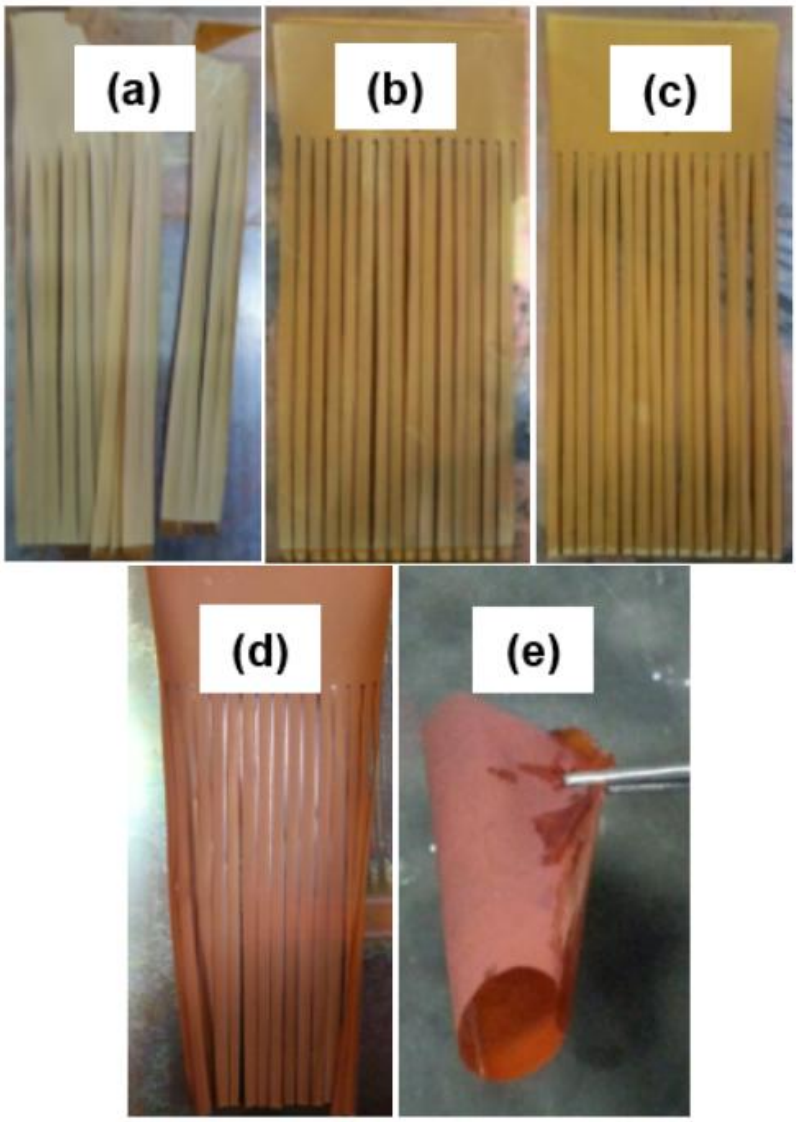

Figure 2-6. Photograph images of (a) BA-a H, (b) BA-a 2 blend H, (c) BA-a 1 blend H, (d) linear polybenzoxazine H and (e) neat linear polybenzoxazine film

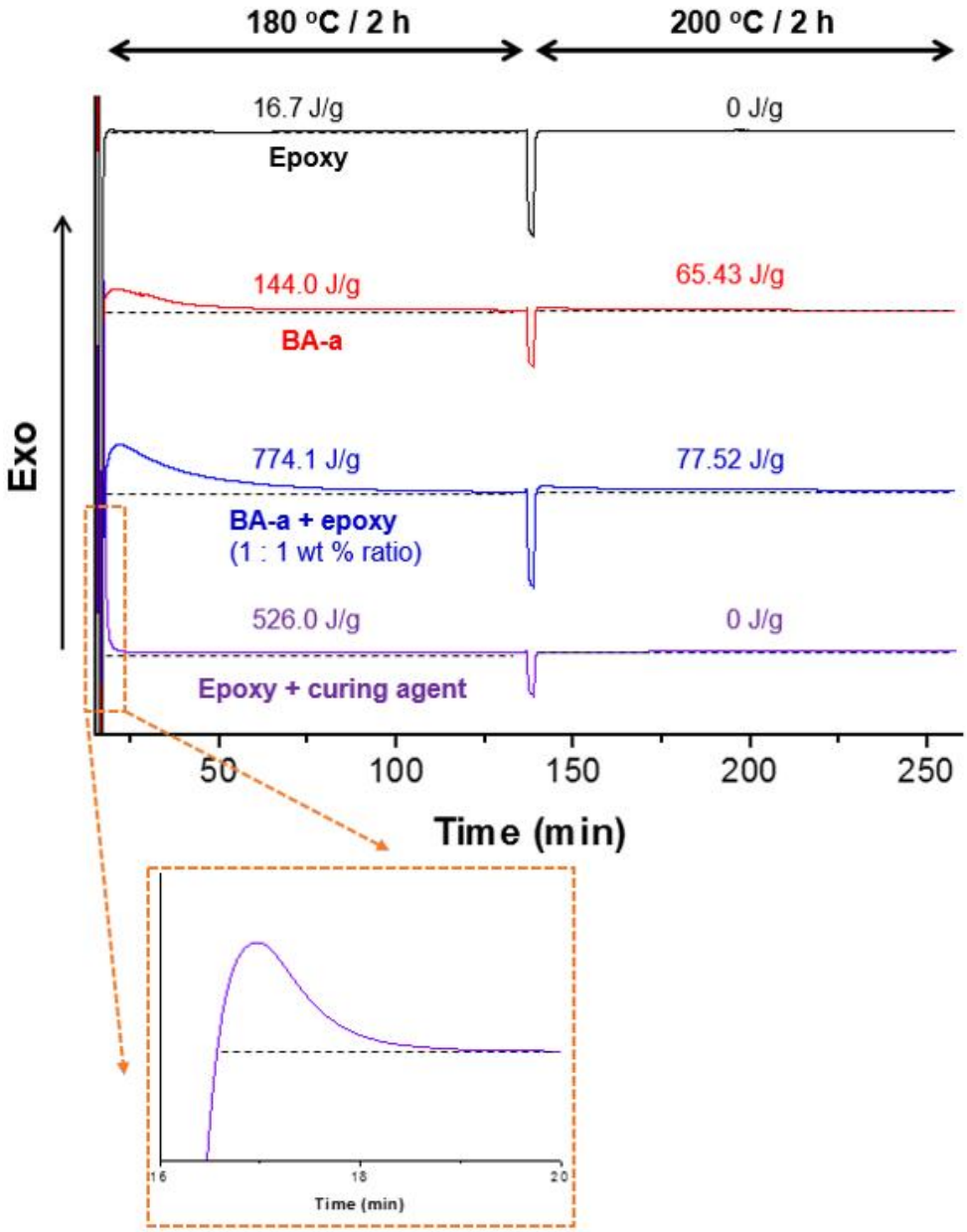

Figure 2-7. DSC trace of epoxy, BA-a and blend system

the isothermal heating at 180 ^{o}C for 2 h and 200 ^{o}C for 2 h. The neat epoxy was barely cross-linked during the heat treatment; on the contrary, the trace of BA-a exhibited the exotherm peak of curing at the beginning of the first heating cycle with the enthalpy of transition of 144.0 J/g. Enthalpy of transition in the case of epoxy resin with curing agent was dramatically increased with the enthalpy of transition of 526.0 J/g, which indicated that the curing agent quickly cross-linked the epoxy rings at the beginning of the cure process. The DSC trace of BA-a/epoxy blend system showed the similar trend with that of BA-a and exhibited the exotherm transition of 774.1 J/g. Thus, the epoxide ring was believed to be fully cross-linked by the presence of the phenol groups generated from curing process of benzoxazine. These results also indicated that epoxy resin and polybenzoxazine were not physically mixed but formed chemically conjugated blend systems.

In order to investigate the feasibility of the hybrid films consisting of benzoxazine, epoxy and silica nanoparticles as a PCB material, dissipation factors were measured and peeling test was conducted with CCL as described in the experimental section. First, the change of dissipation factor according to the chemical structure of monobenzoxazine was

analyzed, which is shown in Table 2-2. The weight ratio of monobenzoxazine to epoxy was 1:1, and the

Table 2-2. Dissipation factor of monobenzoxazine and epoxy/silica hybrid films

Benzoxazine : Epoxy (wt %)	**Dissipation factor**			
	BA-a	**BF-a**	**Hexyl-benzoxazine**	**Dodecyl-benzoxazine**
1 : 1	0.0066 ± 0.0002 (n = 2)	0.0080 ± 0.0005 (n = 2)	0.0068 ± 0.0001 (n = 2)	0.0096 ± 0.0020 (n = 2)

weight ratio of the entire thermosetting resin to silica nanoparticles was 7:3. However, there was no significant different tendency of dissipation factor from 0.0066 to 0.0096 implying that aromatic or aliphatic structure of benzoxazine did not extensively affect dissipation factor. Although there was no tendency to change the dissipation factor depending on the molecular structure of benzoxazine, we continued to select BA-a due to lowest dissipation factor of the BA-a-based hybrid film. The results are summarized in Table 2-3. Dissipation factors of benzoxazine and hybrid films were lower than that of epoxy-based hybrid film which was evaluated as 0.0079. The BA-a H film showed the lowest dissipation factor around 0.0042, but it was so brittle and non-adhesive to copper foil that peeling test could not proceed. The addition of epoxy resin had been reported to have a negative influence on the dissipation factor, however, it was considered indispensable in terms of improvement in mechanical properties and adhesion to CCL. As expected, the dissipation factor increased with increasing the amount of epoxy in BA-a hybrid, but the physical properties were still not good enough to produce reliable results in the peeling test. The dissipation factor of 0.0052 displayed by linear polybenzoxazine H was

slightly higher than that of BA-a H and much lower than that of epoxy. The film made of linear polybenzoxazine relulted dramatic improvement of physical property, but adhesion to copper

Table 2-3. Dissipation factor & brittleness & peel strength of BA-a or linear polybenzoxazine and epoxy/silica hybrid film

Film	Dissipation Factor	Brittleness	Peel strength (kgf / cm^2)
BA-a H[a]	0.0042 ± 0.0001 (n = 2)	Very brittle	N/A[c]
BA-a 2 blend H[b]	0.0059 ± 0.0001 (n = 2)	Very brittle	N/A[c]
BA-a 1 blend H[b]	0.0066 ± 0.0002 (n = 2)	Moderately brittle	N/A[c]
Linear polybenzoxazine H[a]	0.0052 ± 0.0001 (n = 2)	Flexible	N/A[d]
Linear polybenzoxazine 2 blend H[b]	0.0058 ± 0.0001 (n = 2)	Flexible	0.59 ± 0.05 (n = 2)
Linear polybenzoxazine 1 blend H[b]	0.0064 ± 0.0001 (n = 2)	Flexible	0.65 ± 0.04 (n = 2)

[a] Benzoxazine/silica nanoparticles hybrid, [b] Benzoxazine/epoxy/silica nanoparticles hybrid, [c] Due to brittleness, [d]Due to the poor adhesion to copper

Dissipation factor of epoxy/silica hybrid film : 0.0079 ± 0.0001 (n = 2)

foil was limited to be applied as a PCB material. The observation that polybenzoxazine film exhibited lower dissipation factor and non-adhesiveness was in good agreement with the previous reports that the phenol groups formed during the benzoxazine ring opening process participated in the formation of hydrogen bonding inside the benzoxazine system. In order to endow the linear polybenzoxazine-based films with adhesiveness, the epoxy resin was added to hybrid films. The dissipation factors and peel strength to the copper foil of the linear polybenzoxazine hybrids increased with the amount of epoxy resin, but the difference of dissipation factor was not so large as the case of BA-a H. Regardless of the blend ratio, linear polybenzoxazine hybrids showed comparable values of dissipation factor and peel strength, which was improved than epoxy based hybrid systems.

2.4. Conclusion

Benzoxazine-based silica hybrid material was investigated with excellent mechanical properties and improved insulation performance. Previous studies have shown that high temperature was required for complete curing of benzoxazine, but this study found that complete curing was achieved at lower temperatures with proper heat treatment time. The insulation properties of the hybrid films prepared through the chemical structure change of monobenzoxazine were evaluated and showed no significant trend. Among various compositions of benzoxazine and epoxy blend system, hybrid films with higher content of benzoxazine exhibited lower dissipation factor (~ 0.005 frequency/10 GHz). The results support that monobenzoxazine is a new class of potential materials as an excellent electrical insulator, while its hybrid film with silica requires the improvement of the mechanical property. In addition, the linear

polybenzoxazine-based hybrid film exhibited better mechanical strength with a comparable dissipation factor than the blend system of epoxy and monobenzoxazine-based film. For acceptable adhesion to a copper foil, employment of epoxy was necessary for all the hybrid films investigated in this study.

2.5. References

[1] H. Z. Akbas, H. Durmus, G. Ahmetli, *Ozean Journal of Applied Sciences* **2009**, *2*, 443.

[2] M. Pan, C. Zhang, B. Liu, J. Mu, *Journal of Materials Science Research* **2013**, *2*, 153.

[3] R.-H. Lin, W.-H. Lu, C.-W. Lin, *Polymer* **2004**, *45*, 4423.

[4] M. Laskoski, D. D. Dominguez, T. M. Keller, *J. Mater. Chem.* **2005**, *15*, 1611.

[5] J. H. Wang. G. Z. Liang, H. X. Yan, S. B. He, *eXPRESS Polymer Letters* **2008**, *2*, 118.

[6] J.-J. Park, *Trans. Electr. Electron. Mater.* **2012**, *13*, 322.

[7] C. Yan, X. Fan, J. Li, S. Z. Shen, *Journal of Applied Polymer*

Science **2011**, *120*, 1525.

[8] F. W. Holly, A. C. Cope, *J. Am. Chem. Soc.* **1944**, *66*, 1875.

[9] K. Zhang, Q. Zhuang, Y. Zhou, X. Liu, G. Yang, Z. Han, *Journal of Polymer Science: Part A: Polymer Chemistry* **2012**, *50*, 5115.

[10] H.-D. Kim, H. Ishida, *J. Phys. Chem. A*. **2002**, *106*, 3271.

[11] X. Ning, H. Ishida, *Journal of Polymer Science: Part A: Polymer Chemistry* **1994**, *32*, 1121.

[12] B. Kiskan, Y. Yagci, H. Ishida, *Journal of Polymer Science: Part A: Polymer Chemistry* **2008**, *46*, 414.

[13] S. Rimdusit, H. Ishida, *Journal of Polymer Science: Part B: Polymer Physics* **2000**, *38*, 1687.

[14] A. Sudo, L.-C. Du, S. Hirayama, T. Endo, *Journal of Polymer Science: Part A: Polymer Chemistry* **2010**, *48*, 2777.

[15] H. Yeganeh, M. Razavi-Nouri, M. Ghaffari, *Polymer Engineering and Science* **2008**, *48*, 1329.

[16] T. Takeichi, T. Kano, T. Agag, *Polymer* **2005**, *46*, 12172.

[17] Z. Brunovska, J. P. Liu, H. Ishida, *Macromol. Chem. Phys.* **1999**, *200*, 17545.

Chapter 3.

High-Performance Insulating Materials Based on Benzoxazine with Cyano Group Introduced

3.1. Introduction

Printed circuit boards (PCBs) with an electronic circuit on insulator matrixes support and electrically connect electrical components. Single-side PCB, double-side PCB, multi-layer PCB and flexible PCB are divided according to the number of wiring circuit layers [1]. Recently, as the functions of electronic products become complicated and miniaturized, the demand for multi-layer PCBs is increasing. Also, fast speed of the signal transmission and reduction of crosstalk to electronic devices are required. In order to meet these requirements, the electrical insulation performance of the insulating layer should be excellent.

Epoxy, one of the most commercially used thermoset polymer [2], has high polarity hydroxyl groups in the thermosetting process and is not suitable for this requirement owing to its poor insulation performance. Many

polymeric materials are being studied to replace epoxy, for example cyanate ester [3], [4], [5], [6], [7], polyphenylene ether [8], bismaleimide [9], [10] and polydicyclopentadiene [11]. The cyanate esters are polymerized through the thermosetting process in the presence of a catalyst such as transition metal, phenol and water to form polycyanurate with a triazine ring. Polycyanurates are attracting considerable attention as an outstanding material due to their high T_g, low moisture absorption, and electric properties. According to the reported studies, the electronegativity and the dipole concentration are diluted by the large bulkiness of the triazine ring generated from curing process of the cyanate ester, which improves the insulation property. However, since the viscosity increases rapidly at the end of the polymerization process, the cyclotrimerization is incomplete resulting in a low cross-link density, which adversely affects the insulation. Therefore, studies have been reported to enhance the cross-link density by blending with other polymers resulting improvement of the insulation.

In addition, polyphenylene ethers are a highly aromatic polymer with low moisture absorption, high T_g, excellent electrical insulation over a wide temperature range. Polydicyclopentadienes are suitable for PCB materials because of their low polarity properties, low moisture absorption and high T_g. Studies of organic/inorganic hybrid PCB materials were

reported that the introduction of silica nanoparticles increased physical, mechanical, thermal stability and electrical insulation performance [12], [13].

Benzoxazines are high-performance phenolic resins with excellent insulating properties, high T_g, flame-retardant and near-zero volumetric change [14], [15], [16], [17], [18], [19]. Benzoxazines are synthesized by Mannich reaction using various phenols and amines in a short time under bulk or solution conditions. The synthesized benzoxazines are cured through a thermally activated ring-opening process without any catalyst.

In this study, hybrid films containing silica nanoparticles were prepared by blending cyano-benzoxazine [20], [21] and epoxy. Because the single cyano-benzoxazine film exhibited brittle properties, epoxy resin was introduced to increase the physical stability of the film. As a result, the incorporation of cyano group into benzoxazine improved the insulation performance and increased the mechanical strength of the film by introducing epoxy resin. Through this process, optimized hybrid materials with excellent electrical insulation were developed.

3.2. Experimental

Materials. Bisphenol A (99 %), NaOH (98 %) 1,4-dioxane (99.5 %) and chloroform (99.5 %) were obtained from Daejungchem. Paraformaldehyde (95 %), 4-aminobenzonitrile (98 %), 4-dimethylamino pyridine (DMAP, 99 %) and cyclohexanone (99 %) were purchased from Sigma-Aldrich. Epoxy with the trade name of YD-128 (epoxy equivalent weight, EEW: 184~190 g/eq) and phenoxy thermoplastic were kindly received from Kukdo Co., Ltd. PS-6313 (equivalent weight: 148 g/eq), epoxy curing agent, was commercially available from Gun Ei Chemical Industry., Ltd. Leveller with the trade name of BYK 337 was used as received from BYK. Active-ester catalyst, whose trade name is HPC-8000-65T (equivalent weight: 223 g/eq), was acquired by DIC., and silica nanoparticles slurry coated by epoxy was purchased from Admatechs.

Synthesis of Cyano-Benzoxazine. Cyano-benzoxazine was synthesized using the reported method [20]. Bisphenol A (5.0 g, 21.8 mmol), paraformaldehyde (3.2 g, 106.7 mmol) and 4-aminobenzonitrile (5.2 g, 44.0 mmol) were placed in a one-neck round bottom flask equipped with a magnetic stirrer. After equipped in an oil bath heated to 140 ^{o}C, stirring was performed for 1 h. When the reaction was completed, the mixture was cooled to 50 ^{o}C and then dissolved in 25 ml of chloroform. The solution was washed several times with 1 N NaOH and deionized water. Finally, the solution was precipitated in 200 ml diethyl ether, filtered, and dried in a vacuum oven at 25 ^{o}C for 24 h.

Cyano-Benzoxazine blend hybrid film. Cyano-benzoxazine (0.60 g, 1.17 mmol), epoxy (0.60 g), epoxy curing agent (0.10 g, 11.68 phr), active-ester catalyst (0.76 g, 81.90 phr), phenoxy thermoplastic (0.50 g, 10.00 phr), DMAP (6.03 mg, 0.05 mmol), leveller (0.15 g, 1.50 phr), epoxy functionalized silica nanoparticles slurry (6.40 g, 70 wt % of the total reagent mixture) and 0.77 ml cyclohexanone were vigorously stirred in a 70 mL vial and cast on a copper foil with the size of 100 mm×100 mm×0.125 mm. After drying the solvent at 80 ^{o}C for 10 min, the copper foil coated

with the hybrid film was cut to a size of 100 mm×3 mm×0.125 mm. The next step was curing process at 180 ^{o}C for 2 h, 200 ^{o}C for 2 and 250 ^{o}C for 5 h, sequentially. After complete curing, copper foil coated with the hybrid film was dipped in 50 wt % nitric acid aqueous solution to remove copper foil. The obtained hybrid film was washed three times with water and dried at 90 ^{o}C oven for 3 h. Hybrid films with a different weight composition of cyano-benzoxazine and epoxy resin were prepared by the same method as mentioned above. The reagents except for cyano-benzoxazine and epoxy were added to the mixture proportionally to the amount of epoxy. The abbreviated name of Cyano-benzoxazine 1 was prepared with cyano-benzoxazine: epoxy wt % 1:1. As with this abbreviation, Cyano-benzoxazine 2 and Cyano-benzoxazine 3 were 2:1 and 3:1 wt %, respectively.

Instruments. ^{1}H nuclear magnetic resonance (^{1}H NMR) were performed using Advance-300 (Bruker) at 300 MHz frequency in deuterium chloroform. Differential scanning calorimetry (DSC) was carried out with Q10 (TA instrument) at the 10 ^{o}C/min heating rate under N_2 atmosphere. Fourier transform-infrared (FTIR) spectra were carried out using Spectrum

GX-1 spectrometer (Perkin Elmer) with KBr pellets under N_2 purging. Spectra of 400 to 4000 cm^{-1} optical range were obtained with 16 scans. Dissipation factor was measured using resonant cavity type microwave dielectrometer (AET, INC) on the frequency of 10 GHz at 25 ^oC. All the films (100 mm×3 mm×0.125 mm) were dried in a vacuum at 25 ^oC for 24 h before conducting the test.

3.3. Results and Discussion

In this study, silica hybrid films were prepared by changing the compositions of cyano-benzoxazine and epoxy (YD-128) blend. Scheme 3-1 shows the chemical structure of cyano-benzoxazine and epoxy used in this study. Cyano-benzoxazine was prepared with bisphenol A, paraformaldehyde and 4-nitroaniline in bulk as shown in Scheme 3-2. The cyano-benzoxazine synthesized without solvent was washed with 1 N NaOH and deionized water to increase the purity. The yield of cyano-benzoxazine was 46 % as pale yellow powder.

Figure 3-1 shows the ^1H NMR spectrum of synthesized cyano-benzoxazine. Corresponds to -O-CH_2-N- and -Ar-CH_2-N- were appeared at 4.6 and 5.4 ppm respectively, which protons belong to the protons of oxazine ring. The methylene proton of -Ar-CH_2-Ar- were detected at 1.5

ppm. Assuming that the oxazine ring is completely closed, the theoretical ratio of methylene proton in oxazine and methyl proton is 4:6. Accordingly, the ratio of the closed-ring structure was calculated as 71 %.

The black line in Figure 3-2 was a non-isothermal DSC trace of cyano-benzoxazine. The red line was the result after non-isothermal heating with 180 ^{o}C for 2 h and 200 ^{o}C for 2 h. Likewise, the blue line resulted after

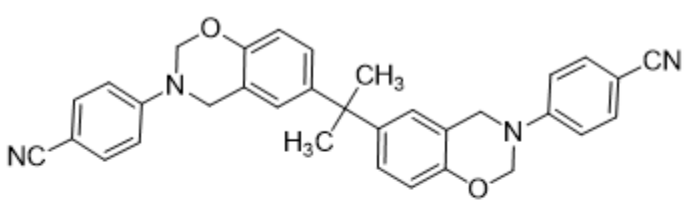

Cyano-benzoxazine

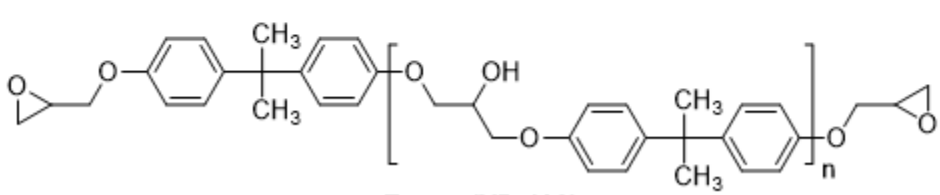

Epoxy (YD-128)

Scheme 3-1. The chemical structure of thermosetting resins

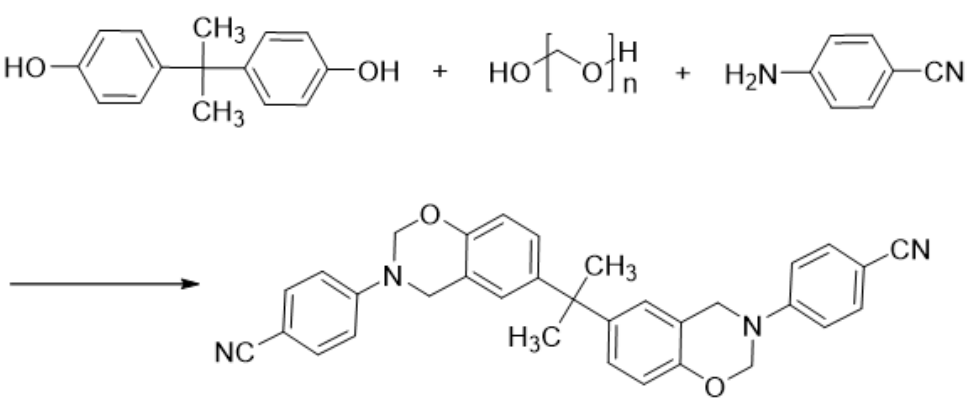

Scheme 3-2. Synthetic method of cyano-benzoxazine

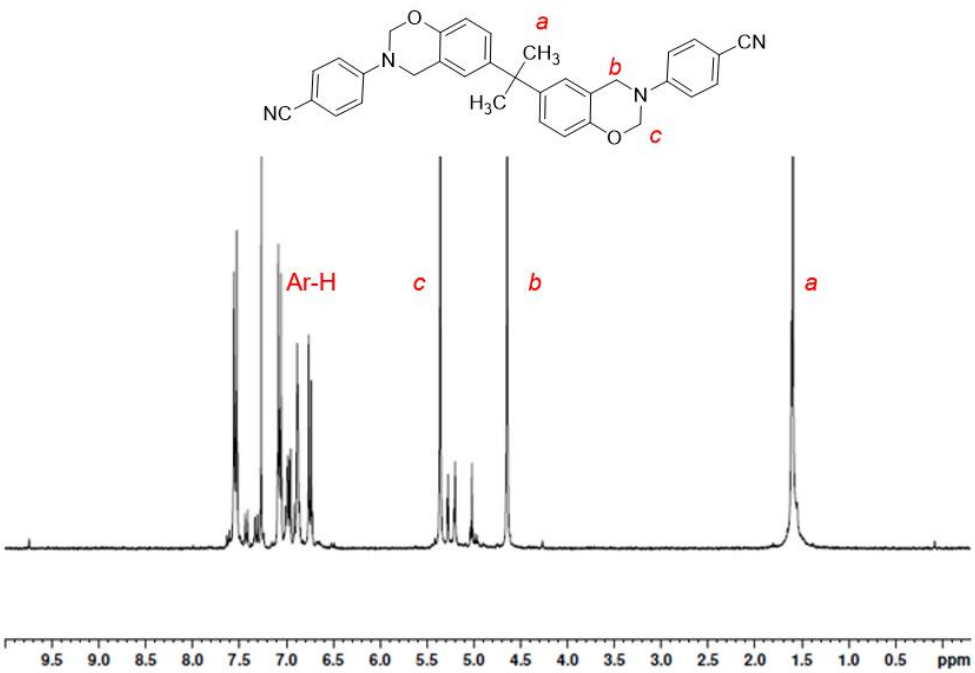
a
CH3
H3C
b
N
O
c
NC
CN
Ar-H
c
b
a
9.5 9.0 8.5 8.0 7.5 7.0 6.5 6.0 5.5 5.0 4.5 4.0 3.5 3.0 2.5 2.0 1.5 1.0 0.5 ppm

Figure 3-1. ^{1}H NMR spectra of cyano-benzoxazine

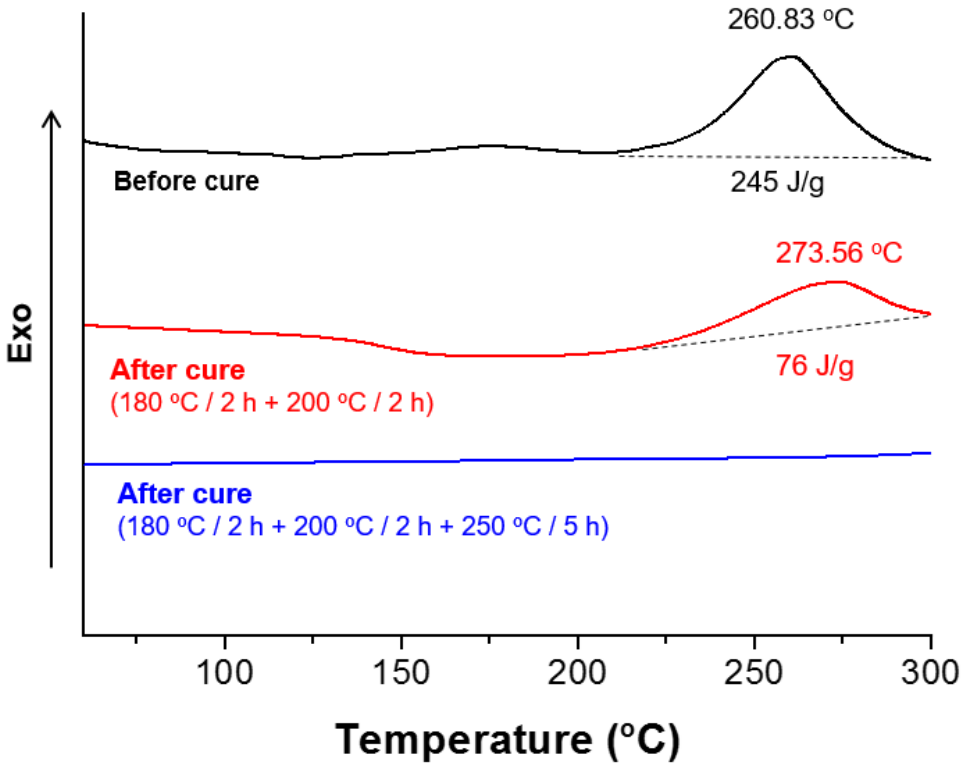

Figure 3-2. DSC trace of cyano-benzoxazine precursors

non-isothermal heating with 180 °C for 2 h, 200 °C for 2 and 250 °C for 5 h, sequentially. Analysis of the DSC trace without isothermal heating resulted in an exotherm peak of 245 J/g at 260.83 °C. DSC trace analysis after

isothermal heating at 180 ^{o}C for 2 h and 200 ^{o}C for 2 h resulted in reduced enthalpy of exothermic transition. After the isothermal heating of 180 ^{o}C for 2 h, 200 ^{o}C for 2 and 250 ^{o}C for 5 h, the oxazine ring and cyano group of cyano-benzoxazine were completely cross-linked. Figure 3-3 shows FTIR spectra before and after isothermal heating of cyano-benzoxazine, respectively. The band at 823 cm^{-1} is assigned to symmetric stretching vibration of C-N-C of the oxazine ring. The absorption at 1232 cm^{-1} corresponds asymmetric stretching vibration of C-O-C of the oxazine ring. The absorption at 3042 cm^{-1} is attributed to the C-H stretching vibration of the aromatic ring. The C-H asymmetric and CH_3 symmetric stretching vibrations are located at 2964 and 2868 cm^{-1}, respectively. The peaks at 1605, 1514 and 1500 cm^{-1} are assigned to the C=C stretching vibrations of the aromatic ring. The absorption at 2220 cm^{-1} is due to the C≡N stretching vibration. After each isothermal heating treatment, FTIR analysis was carried out with the intensity changes of absorption peaks belonged to oxazine ring and C≡N. Two peaks at 1665 and 1582 cm^{-1} formed associated with the C=N stretching vibration of the triazine ring as a result of thermal curing. At the

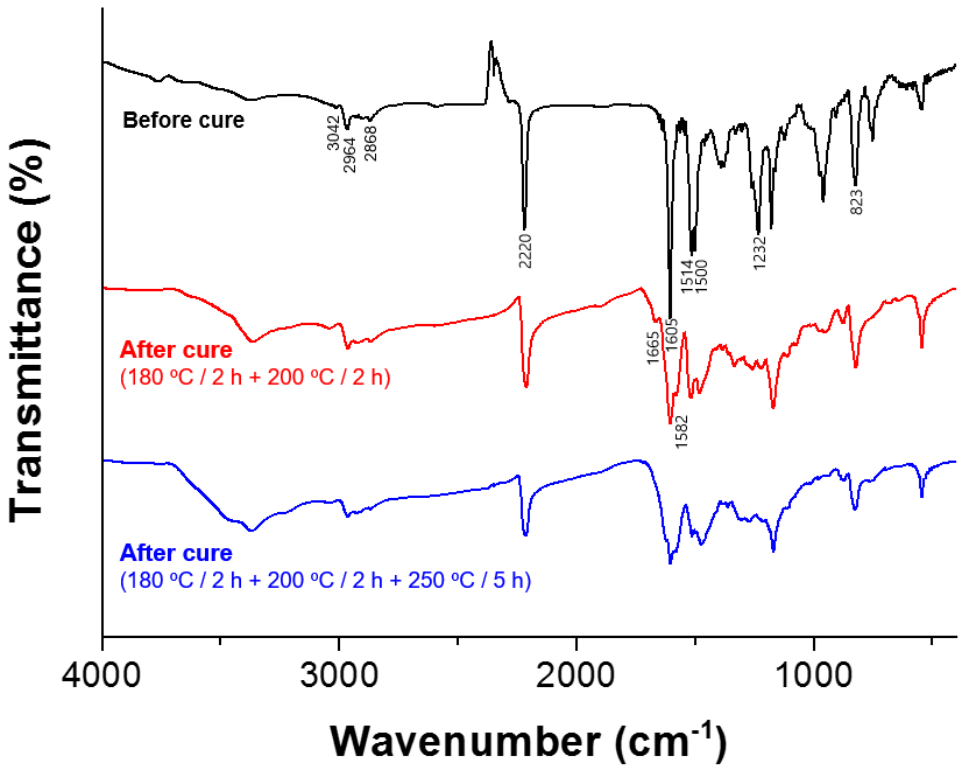

Figure 3-3. FTIR spectra of cyano-benzoxazine precursors

same time, the intensity of peak absorption at 2220 cm^{-1} corresponding to

C≡N decreased. The intensities of absorption peaks at 823 and 1232 cm^{-1} belonged to C-N-C and C-O-C of oxazine ring decreased after isothermal heating, respectively.

Figure 3-4 is a photograph of films prepared with cyano-benzoxazine and epoxy resin, which chemical structures are shown in Scheme 3-2, and silica nanoparticles. To complement the physical property of the hybrid film, the epoxy resin was added to the hybrid composition based on cyano-benzoxazine because polymerized cyano-benzoxazine also showed brittleness as like BA-a. As the content of cyano-benzoxazine in blend mixture was increased, the physical stability of hybrid film was decreased. In this system, cyano-benzoxazine and epoxy blend mixture are chemically bonded by thermosetting, not simple mixing. The chemical structure of cross-linking with epoxy and cyano-benzoxazine are shown in Scheme 3-3.

The dissipation factor was measured to confirm the feasibility of hybrid films made of benzoxazine, epoxy and silica nanoparticles to be applied to PCBs. The results are exhibited in Table 3-1. The dissipation factor of BA-a H was 0.0042. This value was lower than that of epoxy-based hybrid film. Moreover, the dissipation factor of the benzoxazine-

based hybrid film

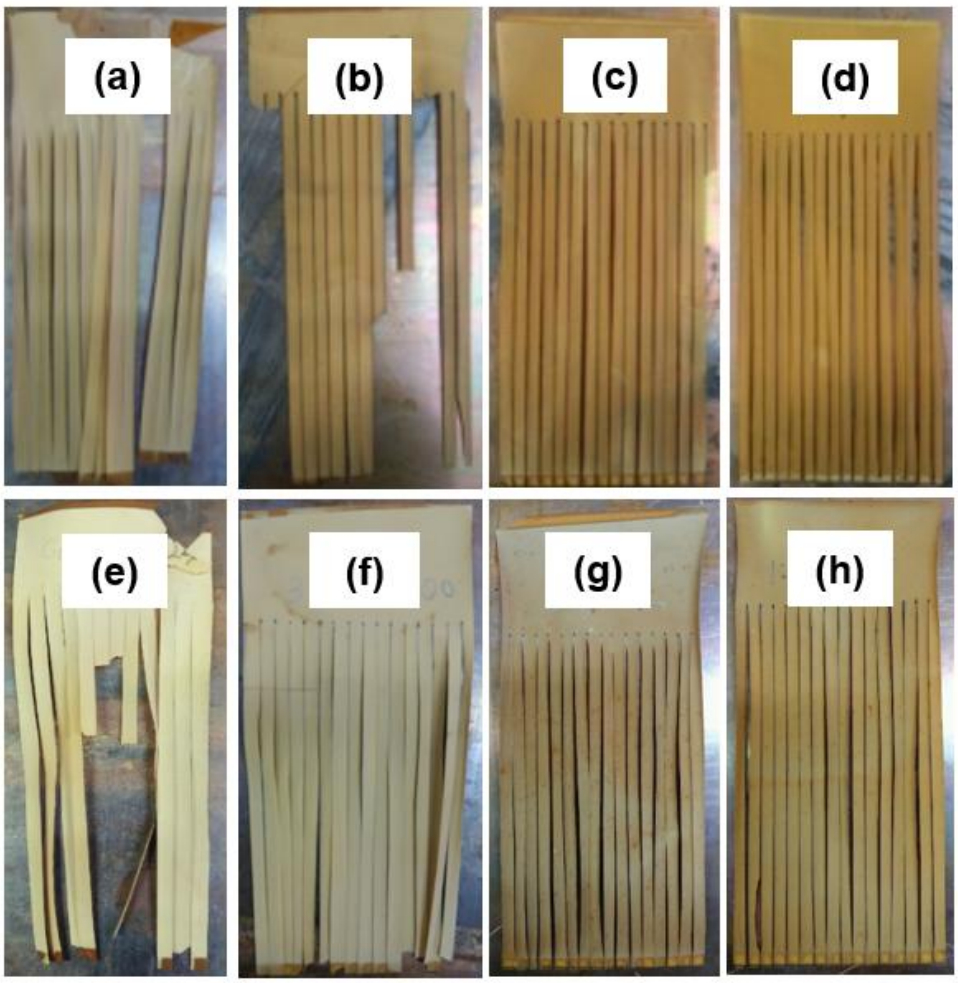

Figure 3-4. Photograph images of (a) BA-a H, (b) BA-a 3 blend H, (c) BA-a 2 blend H, (d) BA-a 1 blend H, (e) cyano-benzoxazine H, (f) cyano-benzoxazine 3 blend H, (g) cyano-benzoxazine 2 blend H and (h) cyano-benzoxazine 1 blend H

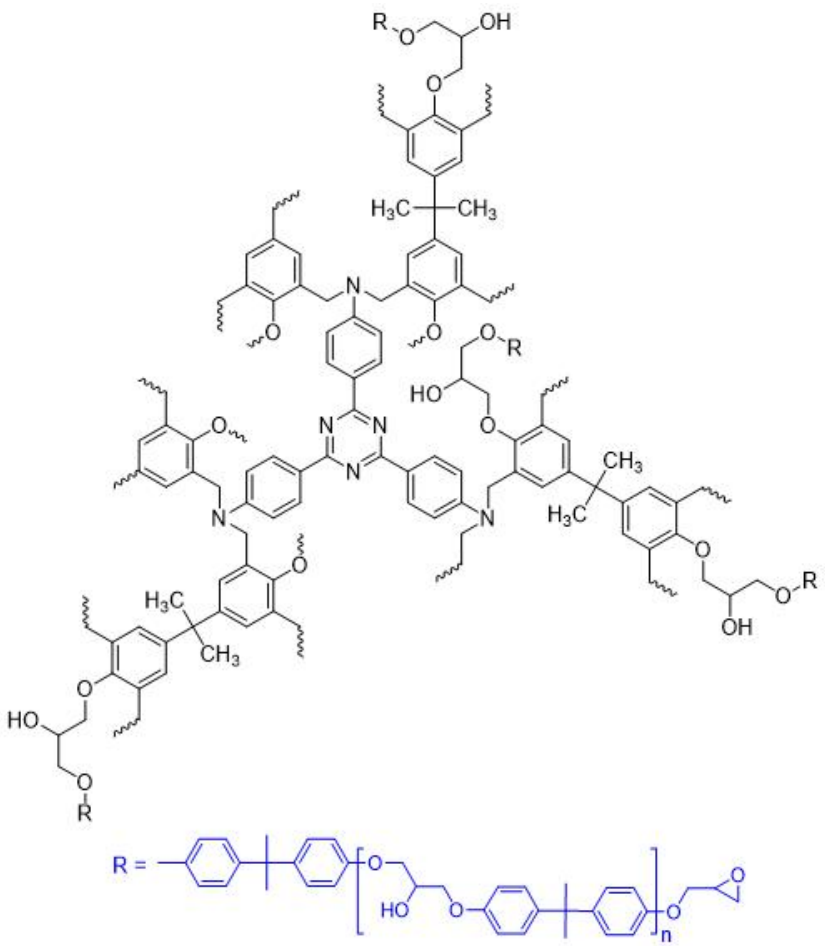

Scheme 3-3. Chemical structure of polymerized cyano-benzoxazine/epoxy blend

Table 3-1. Dissipation factor & brittleness of cyano-benzoxazine or BA-a and epoxy/silica hybrid film

Film	Dissipation Factor	Brittleness
Cyano-benzoxazine H[a]	0.0030 ± 0.0002 (n = 2)	Very brittle
Cyano-benzoxazine 3 blend H[b]	0.0042 ± 0.0002 (n = 2)	Very brittle
Cyano-benzoxazine 2 blend H[b]	0.0053 ± 0.0002 (n = 2)	Very brittle
Cyano-benzoxazine 1 blend H[b]	0.0063 ± 0.0001 (n = 2)	Moderately brittle
BA-a H[a]	0.0042 ± 0.0001 (n = 2)	Very brittle
BA-a 3 blend H[b]	0.0046 ± 0.0003 (n = 2)	Very brittle
BA-a 2 blend H[b]	0.0059 ± 0.0001 (n = 2)	Very brittle
BA-a 1 blend H[b]	0.0066 ± 0.0002 (n = 2)	Moderately brittle

[a] Benzoxazine/silica nanoparticles hybrid, [b] Benzoxazine/epoxy/silica nanoparticles hybrid,

Dissipation factor of epoxy/silica hybrid film : 0.0079 ± 0.0001 (n = 2)

with cyano group was 0.0030, which was lower than that of the BA-a H. Since the triazine ring formed in the thermosetting process of cyano-benzoxazine showed a bulky structure, electronegativity and dipole concentration were diluted. As a result, the reduction of dissipation factor was confirmed. Epoxy resins are known to negatively affect the dissipation factor due to the formation of hydroxyl groups during thermal curing. However, they strengthen the physical stability and the copper adhesion. The results also show that the dissipation factor increased as the addition of epoxy resin but the mechanical strength of the film improved. Overall, the improved dissipation factor was confirmed as cyano group was introduced into benzoxazine.

3.4. Conclusion

Thermosetting polymer/silica nanoparticles hybrid films were investigated as PCB materials with improved dissipation factor. For PCB materials, cyano-benzoxazine was successfully prepared via Mannich reaction employing hydroxyl, amine monomers and paraformaldehyde. Cross-linking is formed through the cyano group as well as the oxazine ring of cyano-benzoxazine with thermal treatment. The triazine formed through the cyclization of the cyano group displays excellent insulation performance since it dilutes the electronegativity, but the thermosetting condition of 250 ^{o}C is required. The DSC and FTIR analyses were performed after high-temperature thermal curing by a sequential rise in temperature, and formation of the triazine ring from cyano group was confirmed through FTIR analysis. Among various compositions of cyano-benzoxazine and epoxy blend system, hybrid films with higher content of cyano-benzoxazine resulted in lower dissipation factor (~ 0.004 frequency/10 GHz). However, cyano-benzoxazine has a brittle property like a BA-a-based hybrid film. In order to compensate the physical properties, modification of the chemical structure such as linear polymerization will have enhanced physical properties and excellent insulation as PCB materials.

3.5. References

[1] A. C. Siegel, S. T. Phillips, M. D. Dickey, N. Lu, Z. Suo, G. M. Whitesides, *Adv. Funct. Mater.* **2010**, *20*, 28.

[2] M. Lé-Magda, E. Dargent, J. A. S. Puente, A. Guillet, E. Font, J.-M. Saiter, *Journal of Applied Polymer Science* **2013**, *130*, 786.

[3] A. Osei-Owusu, G. C. Martin, J. T. Gotro, *Polymer Engineering and Science* **1991**, *31*, 1604.

[4] D. Mathew, C. P. R. Nair, K. Krishnan, K. N. Ninan, *Journal of Polymer Science: Part A: Polymer Chemistry* **1999**, *37*, 1103.

[5] M. Laskoski, D. D. Dominguez, T. M. Keller, *J. Mater. Chem.* **2005**, *15*, 1611.

[6] L. J. Kasehagen, C. W. Macosko, *Polymer International* **1997**, *44*, 237.

[7] J.-Y. Shieh, S.-P. Yang, M.-F. Wu, C.-S. Wang, *Journal of Polymer Science: Part A: Polymer Chemistry* **2004**,42, 2589.

[8] L. Luo, T. Qiu, Y. Meng, L. Guo, J. Yang, Z. Li, X. Cao, X. Li, *RSC Adv.* **2013**, *3*, 14509.

[9] H.-J. Hwang, C.-H. Li, C,-S. Wang, *Polymer* **2006**, *47*, 1291.

[10] R.-H. Lin, W.-H. Lu, C.-W. Lin, *Polymer* **2004**, *45*, 4423.

[11] J.-Y. Shieh, H.-J. Hwang, S.-P. Yang, C.-S. Wang, *Journal of Polymer Science: Part A: Polymer Chemistry* **2005**, *43*, 671.

[12] C. Yan, X. Fan, J. Li, S. Z. Shen, *Journal of Applied Polymer Science* **2011**, *120*, 1525.

[13] J.-J. Park, *Trans. Electr. Electron. Mater.* **2012**, *13*, 322.

[14] H. Ishida, Y. Rodriguez, *Polymer* **1995**, *36*, 3151.

[15] X. Ning, H. Ishida, *Journal of Polymer Science: Part A: Polymer Chemistry* **1994**, *32*, 1121.

[16] S. Rimdusit, H. Ishida, *Journal of Polymer Science: Part B: Polymer Physics* **2000**,38, 1687.

[17] Y.-C. Su, F.-C. Chang, *Polymer* **2003**, *44*, 7989.

[18] P. Velez-Herrera, K. Doyama, H. Abe, H. Ishida, *Macromolecules* **2008**, *41*, 9704.

[19] H. Yeganeh, M. Razavi-Nouri, M. Ghaffari, *Polymer Engineering and Science* **2008**, *48*, 1329.

[20] Y. Liu, S. Zhao, H. Zhang, M. Wang, M. Run, *Thermochimica Acta* **2012**, *549*, 42.

[21] Y. Liu, S. J. Zhang, C. Liao, J. Zheng, S. Zhao, M. Run, *Thermochimica Acta* **2013**, *573*, 138.

Chapter 4.

Research for Thermotropic Liquid Crystalline Polyester

4.1. Introduction

Liquid crystalline polymers have been developed as super engineering plastics displaying excellent mechanical strength, processibility, thermal stability and chemical resistance [1]. With various properties of liquid crystalline polymers, they are widely used in electrical components [2] or fields with high mechanical properties are required.

Typically, the structures of liquid crystalline polymers are composed of benzene rings at *p*- or *m*- positions of ester or amide bonds. The most representative liquid crystalline polymer composed of an amide bond is poly (1,4-phenyleneterephthalamide) so-called Kevlar [3], [4], which exhibits excellent mechanical properties due to its structural characteristics. However, Kevlar has a high melting point and a low solubility in a solvent, resulting in poor processibility. The most basic liquid crystalline polymer of the ester bond is Ekonol [5], which is composed of *p*-hydroxybenzoic acid (*p*-HBA). However, Ekonol has a melting point above 500 ^{o}C and the thermal degradation temperature of 440 ^{o}C resulting drawback of processibility. Vectra A [6] is a commercialized product which is polymerized

with *p*-HBA and 6-Hydroxy-2-naphthoic acid (HNA) to complement the disadvantage of Ekonol.

Thermotropic liquid crystalline polyesters (TLCPs) exhibit a high degree of orientation at temperatures above the melting point and thus have excellent processibility. For this reason, TLCPs exhibit high potential as blend additives and have been reported to be processed with thermoplastic polymers such as polyester [7], [8], nylon [9], and phenoxy [10]. Adding a small amount of TLCPs to thermoplastic polymers results in a highly elongated fibrous structure, which enhances mechanical properties such as strength, toughness and a low coefficient of thermal expansion effect. Also, studies have been reported on mixing two kinds of TLCPs to show new properties [11]. In order to process with these TLCPs and thermoplastics, the difference of the melting point between the TLCPs and thermoplastics should be close. Therefore, it is necessary to adjust the melting point of TLCPs to be applied for the specific purpose. The melting point of TLCPs can be controlled by changing the structure of the monomers such as kink units, *m*-position units, flexible aliphatic units and substituent units [12], [13], [14], [15], [16].

In this study, condensation polymerization was carried out in bulk state using several compositions of *p*-HBA, HNA, resorcinol, 4,4'-biphenol

(BP) and terephthalic acid (TPA). In the first step, the hydroxyl groups of the monomers were activated through acetylation process [17], and the high-molecular-weight TLCPs were obtained by increasing the temperature and reducing the pressure in the next step. The change of melting point was confirmed by adjustment of the content of HNA or resorcinol in the polymerization. The manufactured TLCPs were characterized using differential scanning calorimetry (DSC), melting point apparatus, thermogravimetric analysis (TGA), wide angle x-ray scattering (WAXS) and polarization microscope.

4.2. Experimental

Materials. *p*-Hydroxybenzoic acid (*p*-HBA) (98 %) and terephthalic acid (TPA) (99 %) were purchased from Junsei. 6-Hydroxy-2-naphthoic acid (HNA) (98 %) was obtained from TCI. 4,4'-Biphenol (BP) (99 %) was kindly received from Songwon. Acetic anhydride (96 %) and resorcinol (98 %) were commercially available and used as received from Daejungchem. Potassium acetate (99 %) was received from Sigma-Aldrich.

Determination of Reaction Condition. The polymerization of TLCPs proceeded through acetylation, oligomerization and polymerization sequentially. For the first step, acetylation was carried out for 3 h, including the temperature ramp up to 140 ^{o}C. The oligomerization process was carried out for 3 h to 3 h 30 min by raising the temperature of 30 ^{o}C higher than the melting point of the oligomer produced during the reaction. The polymerization process was carried out for 30 min at the final temperature

condition of the oligomerization step. The pressure was gradually reduced to 1 torr during this step to obtain the high-molecular-weight of TLCP.

Polymerization of TLCP Based on HBA-BP-Resorcinol-TPA. Three different compositions of HBA-BP-resorcinol-TPA were polymerized to obtain TLCPs [18]. The mol ratio of HBA:BP:resorcinol:TPA was 60:10:10:20 (Resorcinol 10), 60:5:15:20 (Resorcinol 15) and 60:0:20:20 (Resorcinol 20), respectively. Typically, Resorcinol 10 was prepared as follows. *p*-HBA (200.00 g, 1.45 mol), BP (44.94 g, 0.24 mol), resorcinol (26.57 g, 0.24 mol), TPA (80.19 g, 0.48 mol), acetic anhydride (258.29 g, 2.53 mol) g and potassium acetate (61 mg, 0.01 phr) were added to a 1 L separable reaction vessel. The reactor, equipped with impeller containing the mixture, was placed in a heating mantle and stirred using a high torque-type overhead stirrer. For the acetylation process, the reactor was heated to 140 ^{o}C over 1 h and then stirred for 2 h. In this process, the reflux condenser was installed to prevent external leakage of acetic anhydride and acetic acid. After the acetylation process, the reactor was heated to 320 ^{o}C to proceed oligomerization of the monomer for 3 h 30 min. In this procedure, the reflux condenser was removed and the produced acetic anhydride was allowed to

release out. At the end of the reaction, the formation of acetic acid was stopped to some extent, which indirectly confirmed the termination of oligomerization. Finally, for the polymerization process, the reactor was gradually decompressed using a vacuum oil pump until a pressure of 1 torr. Finally, the high-molecular-weight of TLCP was completely prepared over a 30 min decompression. Resorcinol 15 and Resorcinol 20 were also prepared by the above polymerization method.

Polymerization of TLCP Based on HBA-HNA-Resorcinol-TPA. Polymerization of 6 different mol ratios of HBA-HNA-resorcinol-TPA was carried out. The mol ratio of HBA:HNA:resorcinol:TPA was 61:3:18:18 (NR 3/18), 59:5:18:18 (NR 5/18) and 65:5:15:15 (NR 5/15), respectively. For NR 3/18, *p*-HBA (200.00 g, 1.448 mol), HNA (13.40 g, 0.071 mol), resorcinol (47.02 g, 0.423 mol), TPA (70.27 g, 0.423 mol), acetic anhydride (254.46 g, 2.492 mol) and potassium acetate (59 mg, 0.01 phr) were added to a 1 L separable reaction vessel. Experimental conditions for the reactor installation and acetylation process were same as described above. During the oligomerization process, the temperature of the reactor was gradually increased to 275 ^{o}C over 3 h. Finally, the TLCP was obtained by a

polymerization process in which the pressure was reduced to 1 torr at 290 ^{o}C for 30 min. The other compositions of TLCPs based on HBA-HNA-resorcinol-TPA were also polymerized as above method.

Preparation of TLCP Powder. The measurements of WAXS and melting point apparatus were carried out by placing sample powder in a glass capillary tube, which powder was prepared using a cryogenic freezer mill. To prepare the powder, a vial containing 3 g of TLCP sample was equipped in a chamber wound on a magnetic field induction coil. The chamber was immersed in a liquid nitrogen bath and a magnetic field was formed when the electric power was supplied. The steel impactor, which was placed with the TLCP sample inside the vial, was vigorously moved to the left and right by the magnetic field, and the sample was crushed to be TLCP powder with size of smaller than 100 μm.

Instruments. ^{1}H nuclear magnetic resonance (^{1}H NMR) were carried out using Advance-300 (Bruker) at 300 MHz frequency in deuterium DMSO. Differential scanning calorimetry (DSC) was performed with Q 10 (TA instrument) at a heating (and cooling) rate of 10 ^{o}C under N_2 purging. The optical texture of the sample was measured using a polarization

microscope (Leica MPS 30) with a hot-stage. The sample was placed on a glass plate, covered with a cover glass, and melted using a hot-stage to form a sandwich with a thin film inside. The temperature was increased above the melting point of the sample to confirm liquid crystallinity. Wide-angle X-ray scattering (WAXS) was taken with D8 Discover (Bruker) over a temperature range from 250 to 330 ^{o}C at a wavelength of 1.54056 nm. Thermogravimetric analysis (TGA) was measured with Q 50 (TA instrument) at the 10 ^{o}C/min heating rate under N_2 atmosphere. Melting point apparatus, whose trade name is SMP 10 (Bibby sterilin), was used to indirectly confirm the melting point of the TLCP samples. The sample powder was placed in a 2 mm diameter capillary tube and visually confirmed. All TLCP powder was prepared via the Freezer mill 6770 (SPEX). Mechanical properties were measured by Instron Model 5565 with dog-bone shaped specimens (ASTM D 638). The crosshead speed was 5 mm/min at room temperature. The obtained mechanical values represent the average of at least 5 measurements.

4.3. Results and Discussion

TLCPs based on totally aromatic copolyester were prepared with *p*-HBA, HNA, resorcinol, BP and TPA by condensation polymerization. The monomers used in the polymerization and the polymers obtained after polymerization are shown in Scheme 4-1. To activate hydroxyl groups of monomers, acetylation was performed as the first step using acetic anhydride. For the second step, oligomerization was carried out and the generated acetic acid was removed. In the third step, polymerization was proceeded under reduced pressure to 1 torr at a temperature of 30 ^{o}C higher than the oligomer to obtain high-molecular-weight TLCPs.

^{1}H-NMR analysis was performed to determine whether the hydroxyl groups of *p*-HBA, HNA, resorcinol and BP were completely acetylated after 3 h of reaction with acetic anhydride in the presence of potassium acetate as a catalyst. This is shown in Figure 4-1. After acetylation of *p*-HBA, proton peaks of 6.8 and 7.8 ppm were completely

disappeared and new peaks appeared. Peak *a*' was corresponding to the proton of the acetylated monomer and peak *a*" was belong to the dimer. Similarly, acetylation analysis of HNA showed that the *b* peak was completely disappeared and peaks of acetylated monomer and dimer were analyzed. Analysis of resorcinol and BP also

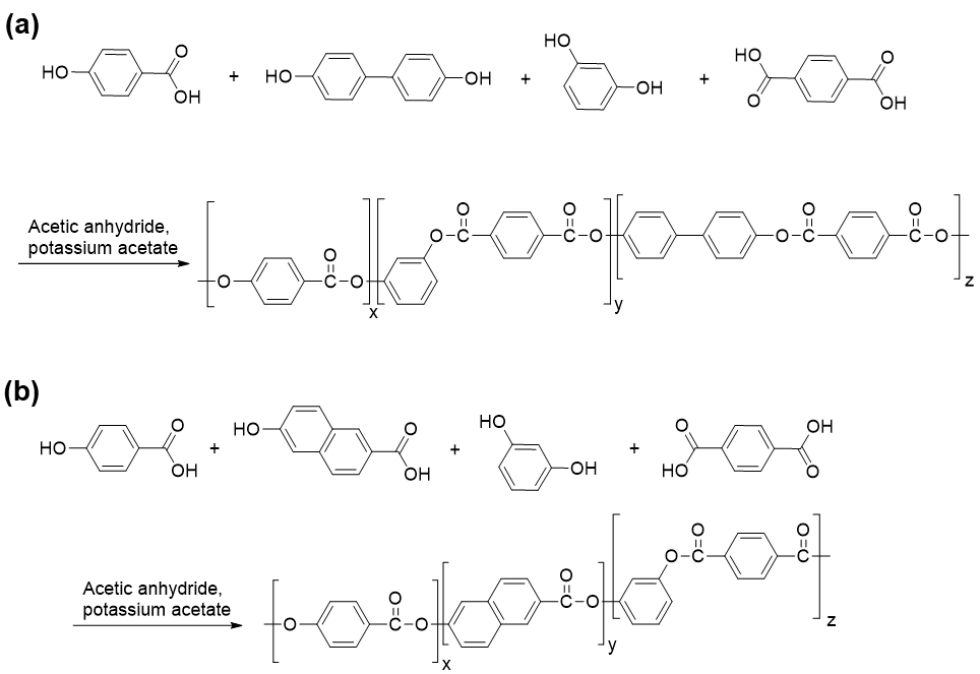

Scheme 4-1. Chemical structure based on (a) HBA-BP-resorcinol-TPA and

(b) HBA-HNA-resorcinol-TPA

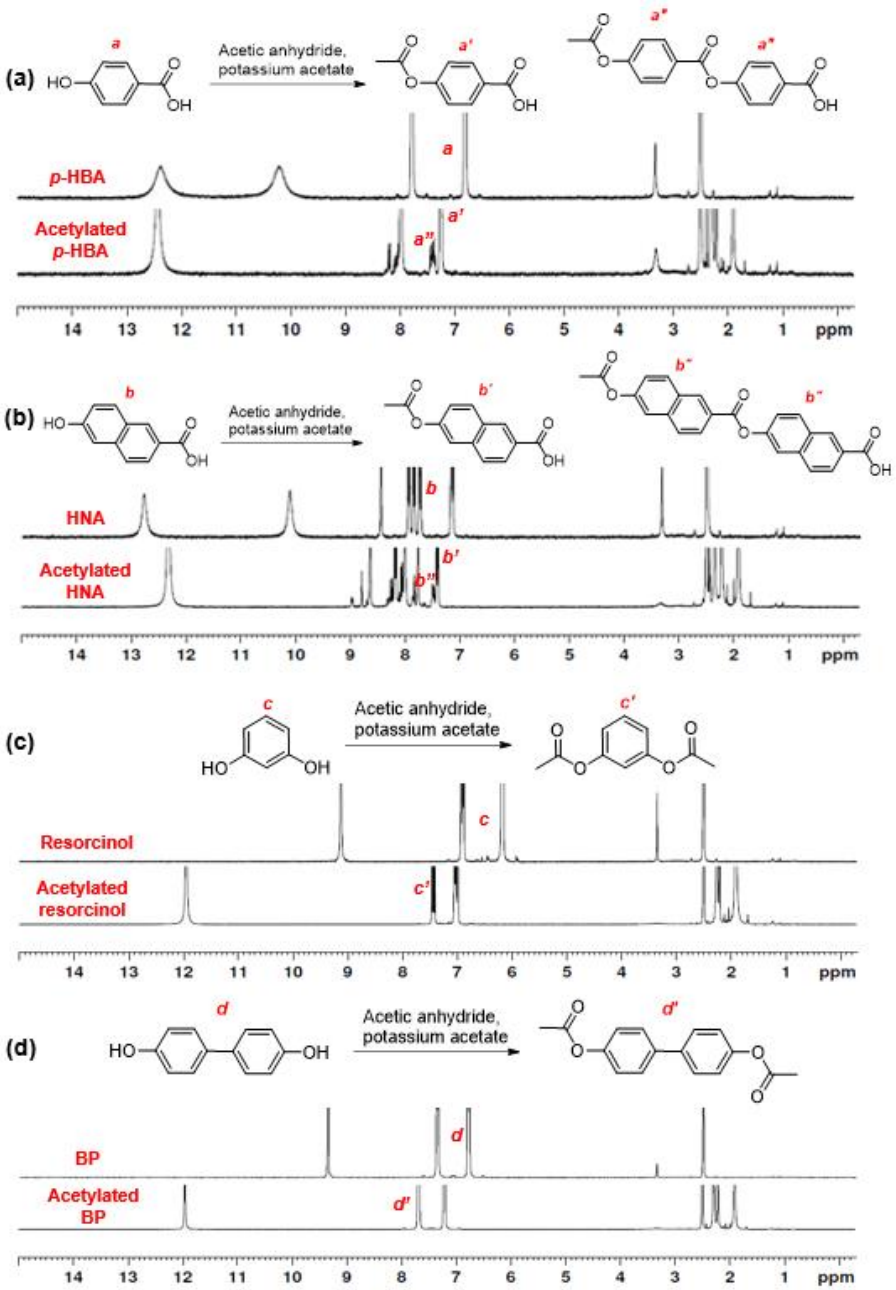

Figure 4-1. Acetylation of *p*-HBA, HNA, resorcinol and BP

showed the disappearance of peaks *c* and *d* after acetylation reaction and new proton peaks *c*' and *d*' were produced. Through these results, it was confirmed that the monomers were fully activated through 3 h of acetylation reaction.

Figure 4-2 shows the DSC trace of Resorcinol 10, Resorcinol 15 and Resorcinol 20 with a heating (and cooling) rate of 10 ^{o}C/min under N_2 atmosphere. The first cooling of Resorcinol 10 resulted in an exothermic transition peak at 246.8 ^{o}C and the second heating analysis showed the enthalpy of endothermic transition at 297.1 ^{o}C. Similarly, in the first cooling step of Resorcinol 15, an exothermic transition peak was observed at 238.5 ^{o}C. However, no peak was observed during the second heating process. In Resorcinol 20, the no-transition peak was observed in the first cooling and second heating. In addition, DSC analysis of NR 3/18, NR 5/18 and NR 5/15 was performed but no-transition peak was observed. TLCPs have a drawback in DSC observations because solid polymers retain their crystallinity when they melt and change into the liquid phase. Therefore, the melting point apparatus was used to observe visually the melting of polymers in the capillary.

Figure 4-3 shows photo images of Resorcinol 10, Resorcinol 15 and

Resorcinol 20, which are HBA-BP-resorcinol-TPA-based polymers. The

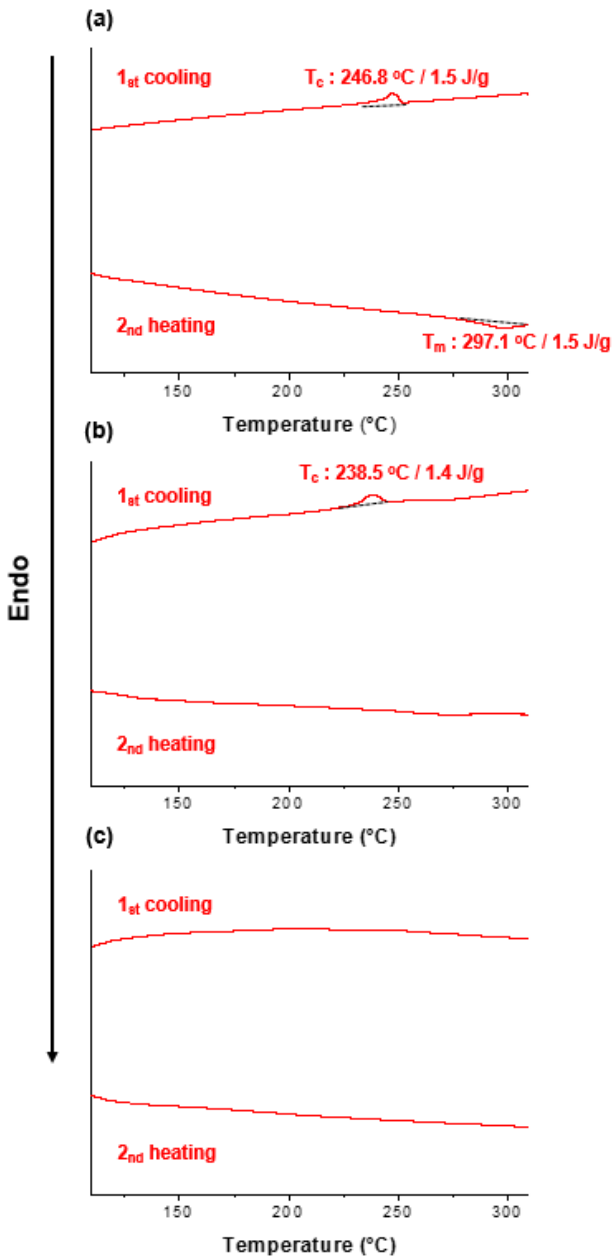

Figure 4-2. DSC trace of (a) Resorcinol 10, (b) Resorcinol 15 and (c) Resorcinol 20

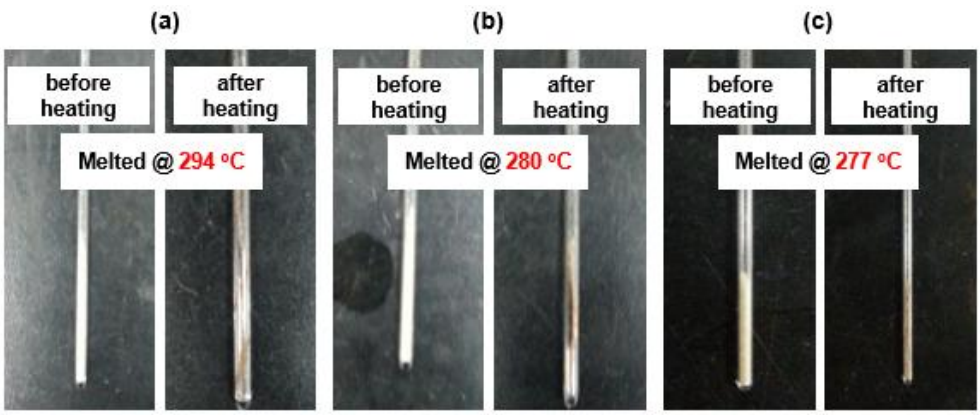

Figure 4-3. Photo images of (a) Resorcinol 10, (b) Resorcinol 15 and (c) Resorcinol 20 (taken by melting point apparatus)

melting point of Resorcinol 10 was visually confirmed to be similar to that of DSC analysis at about 294 ^{o}C. As the content of resorcinol increased for processibility, the melting point of the polymer decreased (see Table 4-1). Figure 4-4 exhibits the photo images of HBA-HNA-resorcinol-TPA-based TLCPs. The melting points were changed by controlling the content of HNA and resorcinol. Comparing NR 3/18 with NR 5/18, the melting point was decreased about 9 ^{o}C as the mol ratio of HNA increased by 2 mol %. Comparing NR 5/18 with NR 5/15, the melting point was increased as resorcinol decreased about 15 ^{o}C as the mol ratio of resorcinol reduced by 3 mol %. Similar to the previous results, the melting point decreased with increasing the content of HNA and resorcinol (see Table 4-2). Thermal stability of Resorcinol 10, 15 and 20 was measured with TGA under N_2 atmosphere at a heating rate of 10 ^{o}C as exhibited Figure 4-5. 5 wt % reduction of all polymers occurred above 400 ^{o}C and Resorcinol 10 showed the highest thermal stability (see Table 4-1). Likewise, TGA analysis of NR 3/18, NR 5/18 and NR 5/15 was performed as shown in Figure 4-6. The 5 wt % reduction of all polymers was observed at over 400 ^{o}C, and NR 3/18

was the most thermally stable (see Table 4-2). The crystallinity of polymers was analyzed by temperature change from 250 to 330 ^{o}C. Table 4-3 shows the WAXS patterns of Vectra A, a commercially available TLCP. As raising

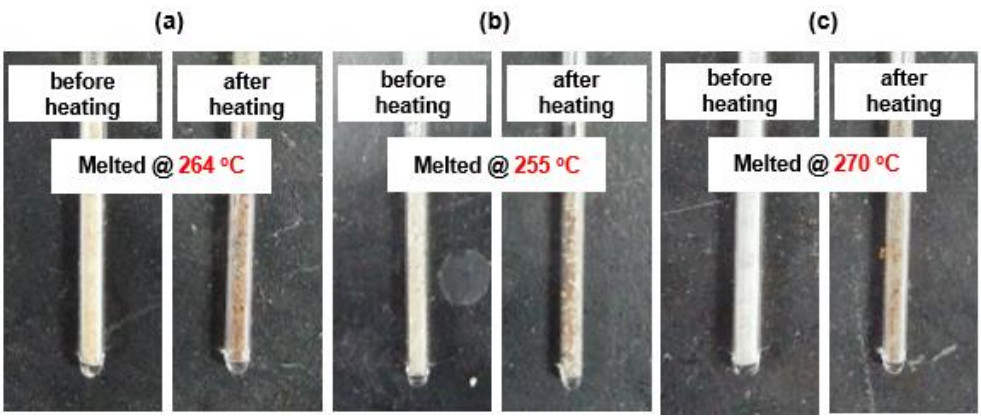

Figure 4-4. Photo images of (a) NR 3/18, (b) NR 5/18 and (c) NR 5/15 (taken by melting point apparatus)

Table 4-1. Thermal properties based on HBA-BP-resorcinol-TPA

Polymer	HBA : BP : Resorcinol : TPA mol ratio	T_c[a]	T_m[b]	T_m[c]	T_d[d]	Liquid crystallinity[e]
Resorcinol 10	60 : 10 : 10 : 20	246.8 °C	297.1 °C	294 °C	488 °C	O
Resorcinol 15	60 : 5 : 15 : 20	238.5 °C	-	280 °C	477 °C	O
Resorcinol 20	60 : 0 : 20 : 20	-	-	277 °C	431 °C	O

[a] The temperatures were measured by DSC at a cooling rate of 10 °C under N_2 atmosphere (first cooling).

[b] The temperatures were measured by DSC at a heating rate of 10 °C under N_2 atmosphere (second heating).

[c] The temperatures were visibly measured by melting point apparatus.

[d] The temperatures at 5 wt % loss of polymer were measured with TGA at a heating rate of 10 °C under N_2 atmosphere.

[e] The liquid crystallinity was measured by X-ray generator and polalization microscope.

Table 4-2. Thermal properties based on HBA-HNA-resorcinol-TPA

Polymer	HBA : HNA : Resorcinol : TPA mol ratio	T_c[a]	T_m[b]	T_m[c]	T_d[d]	Liquid crystallinity[e]
NR 3/18	61 : 3 : 18 : 18	-	-	264 °C	453 °C	O
NR 5/18	59 : 5 : 18 : 18	-	-	255 °C	448 °C	O
NR 5/15	65 : 5 : 15 : 15	-	-	270 °C	430 °C	O

[a] The temperatures were measured by DSC at a cooling rate of 10 °C under N_2 atmosphere (first cooling).

[b] The temperatures were measured by DSC at a heating rate of 10 °C under N_2 atmosphere (second heating).

[c] The temperatures were visibly measured by melting point apparatus.

[d] The temperatures at 5 wt % loss of polymer were measured with TGA at a heating rate of 10 °C under N_2 atmosphere.

[e] The liquid crystallinity was measured by X-ray generator and polalization microscope.

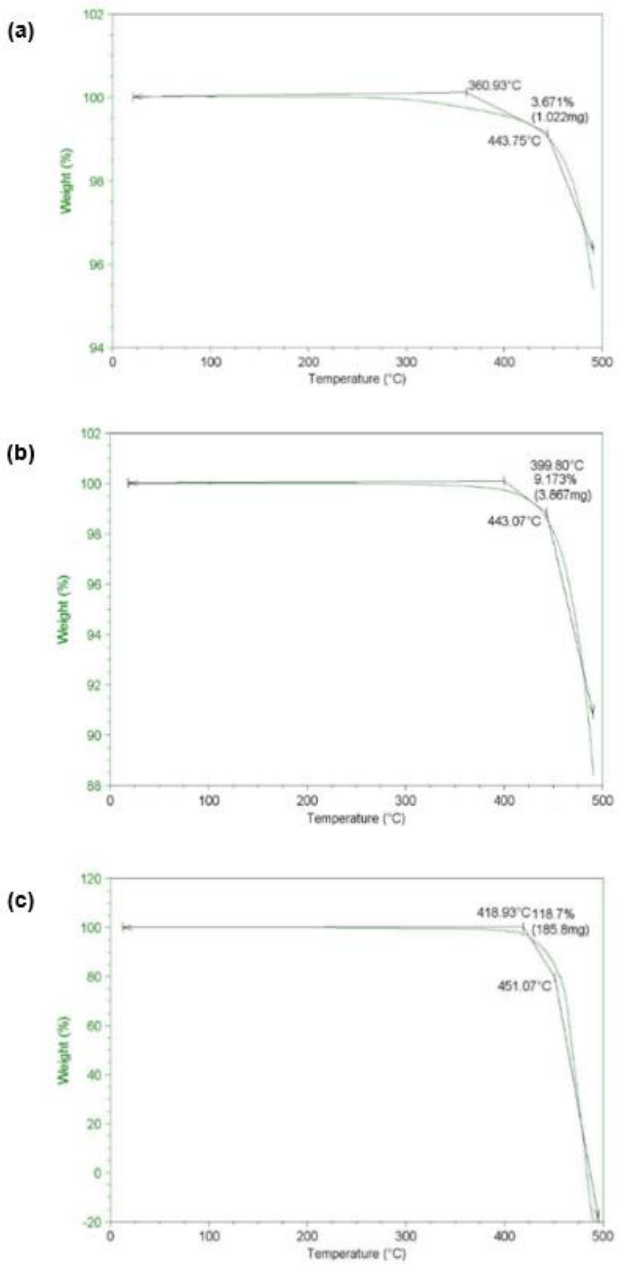

Figure 4-5. TGA curves of (a) Resorcinol 10, (b) Resorcinol 15 and (c) Resorcinol 20

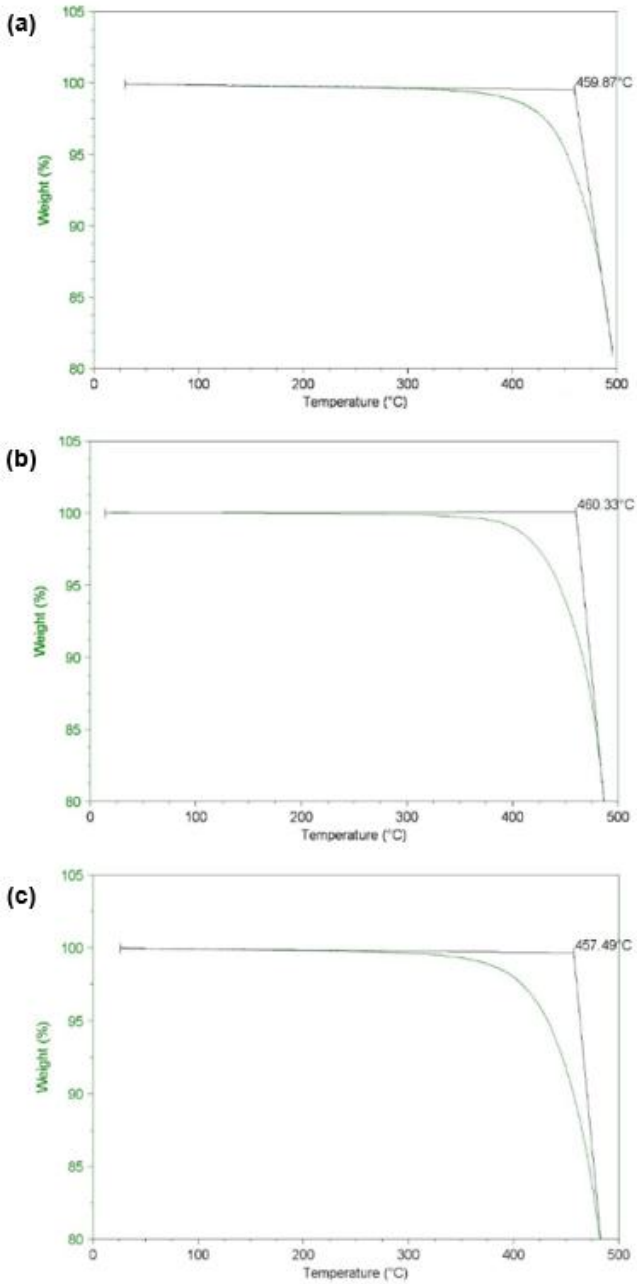

Figure 4-6. TGA curves of (a) NR 3/18, (b) NR 5/18 and (c) NR 5/15

Table 4-3. WAXS data of Vectra A

Polymer	Temperature	2θ	Intensity (%)	d-spacing (Å)	FWHM
Vectra A	250 °C	18.42	100	4.71	8.83
	270 °C	18.20	99	4.87	7.85
	290 °C	18.22	99	4.86	7.10
	310 °C	18.22	99	4.86	8.00
	330 °C	18.22	99	4.86	8.06

temperature above the melting point until 330 °C, Vectra A, which has a melting point of 280 °C and an isotropic temperature of above 500 °C, showed constant sharp peaks intensity at around $2\theta \cong 18$ ° and the *d*-spacing values around 4.7 Å. Through these data, we confirmed the liquid crystallinity of the polymer. Since the crystal structure of Vectra A did not change at temperatures ranging from 250 to 330 °C, full width at half maximum (FWHM) maintained without change. The liquid crystal properties of the following polymers were analyzed through this experimental procedure. All Polymers exhibited liquid crystalline behavior. Figure 4-7 shows the WAXS patterns of Resorcinol 10 with a temperature range from 250 to 330 °C. Resorcinol 10, which had a melting point of 297.1 °C measured by DSC, showed constant WAXS patterns before and after melting point. As shown in Figure 4-8, WAXS patterns of Resorcinol 10, 15 and 20 were measured according to the temperature change and it was confirmed that the tendency of all peaks was constant with an increase in temperature. Table 4-4 illustrates the Bragg angles, *d*-spacing values and FWHM for HBA-BP-resorcinol-TPA-based polymers. Resorcinol 10 had a sharp peak at around $2\theta \cong 19$ ° and *d*-spacing values of 4.68 ~ 4.73 Å before and after melting point of the polymer. The results of FWHM also show that the polymer was liquid crystalline due to no significant change as

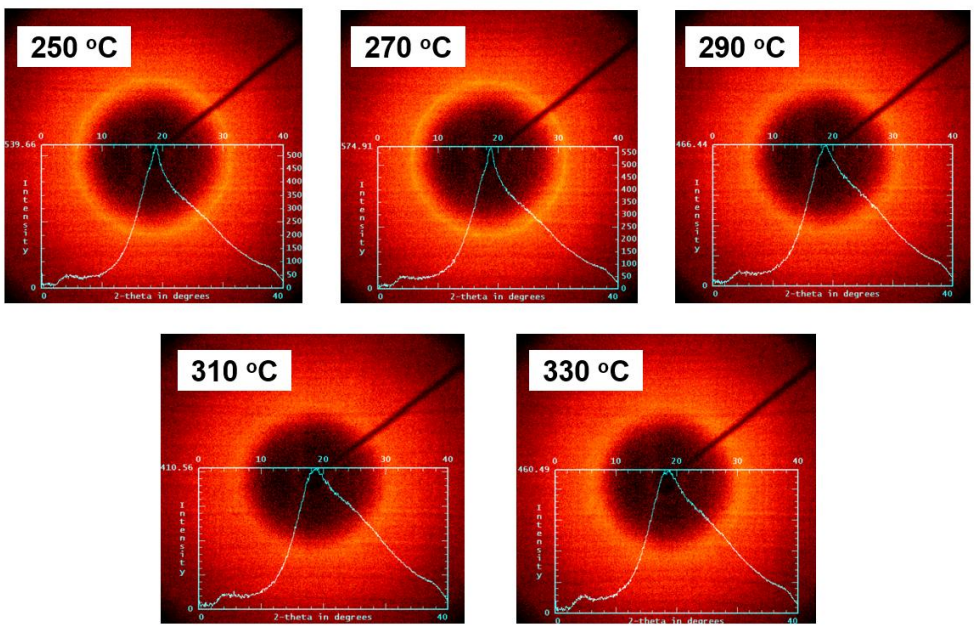

Figure 4-7. WAXS patterns of Resorcinol 10

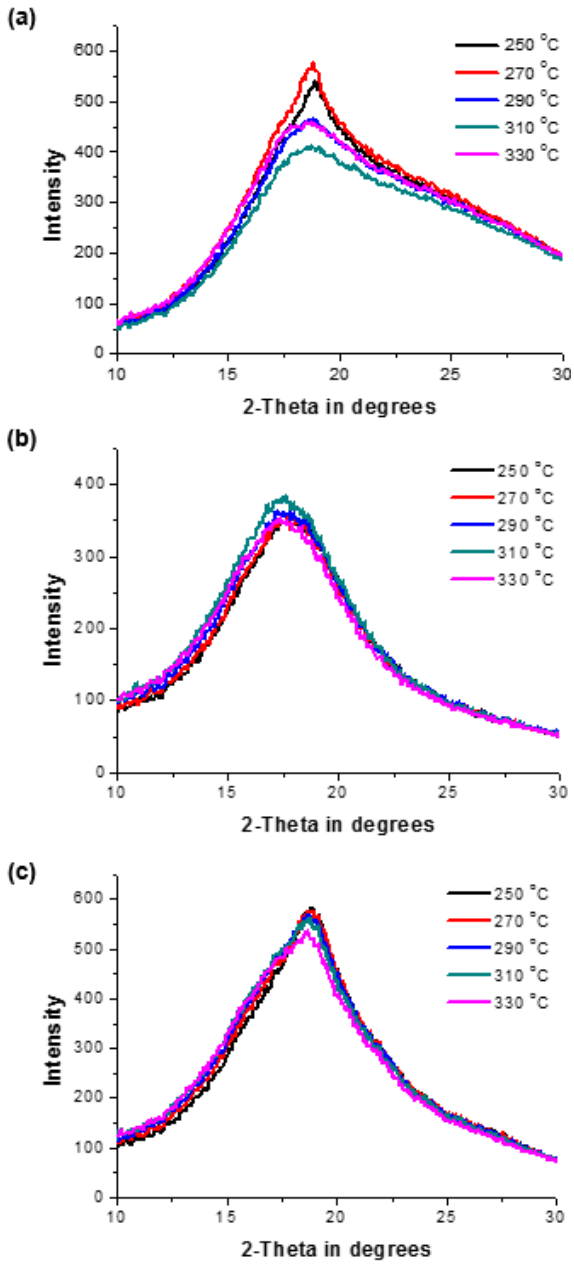

Figure 4-8. WAXS patterns of (a) Resorcinol 10, (b) Resorcinol 15 and (c) Resorcinol 20

Table 4-4. WAXS data based on HBA-BP-resorcinol-TPA

Polymer	Temperature	2θ	d-spacing (Å)	FWHM
Resorcinol 10	250 °C	18.96	4.68	11.20
	270 °C	18.84	4.71	10.80
	290 °C	18.88	4.70	13.05
	310 °C	18.74	4.73	14.25
	330 °C	18.76	4.73	13.97
Resorcinol 15	250 °C	17.80	4.98	15.40
	270 °C	17.72	5.00	14.97
	290 °C	17.80	4.98	15.30
	310 °C	17.58	5.04	14.98
	330 °C	17.66	5.02	15.08
Resorcinol 20	250 °C	18.82	4.71	8.52
	270 °C	18.82	4.71	8.53
	290 °C	18.74	4.73	8.80
	310 °C	18.74	4.73	9.18
	330 °C	18.76	4.73	9.12

the temperature changed. Likewise, Resorcinol 15 and Resorcinol 20 were analyzed and showed liquid crystallinity. Figure 4-9 exhibits that all polymers (NR 3/18, NR 5/18 and NR 5/15) had similar results of liquid crystallinity. All polymers showed sharp peaks at around 18 ~ 20 ^{o}. These results are summarized in Table 4-5. In the temperature range of 250 to 330 ^{o}C, *d*-spacing values of all polymers were confirmed less than 5 Å and FWHM maintained without relatively large variations. These results indicate that all polymers had the properties of TLCPs. Studies on the change of liquid crystallinity with temperature were reported by other researchers [19], [20].

TLCPs behaviors were analyzed by the polarization microscope equipped with hot-stage as exhibited in Figure 4-10 and 4-11. All polymers retained liquid crystallinity even after each melting point and displayed liquid crystal behaviors when the hot-stage temperature was increased to 370 ^{o}C. In Figure 4-10, Resorcinol 10, 15 and 20 represent polished textures in the molten state. Likewise, NR 3/18, NR 5/18 and NR 5/15 were confirmed as liquid crystalline polyester owing to polished textures in Figure 4-11. When all polymers were heated to 370 ^{o}C using a hot-stage, it was confirmed that all polymers exhibited isotropic temperature at least 370

°C because polished textures were maintained.

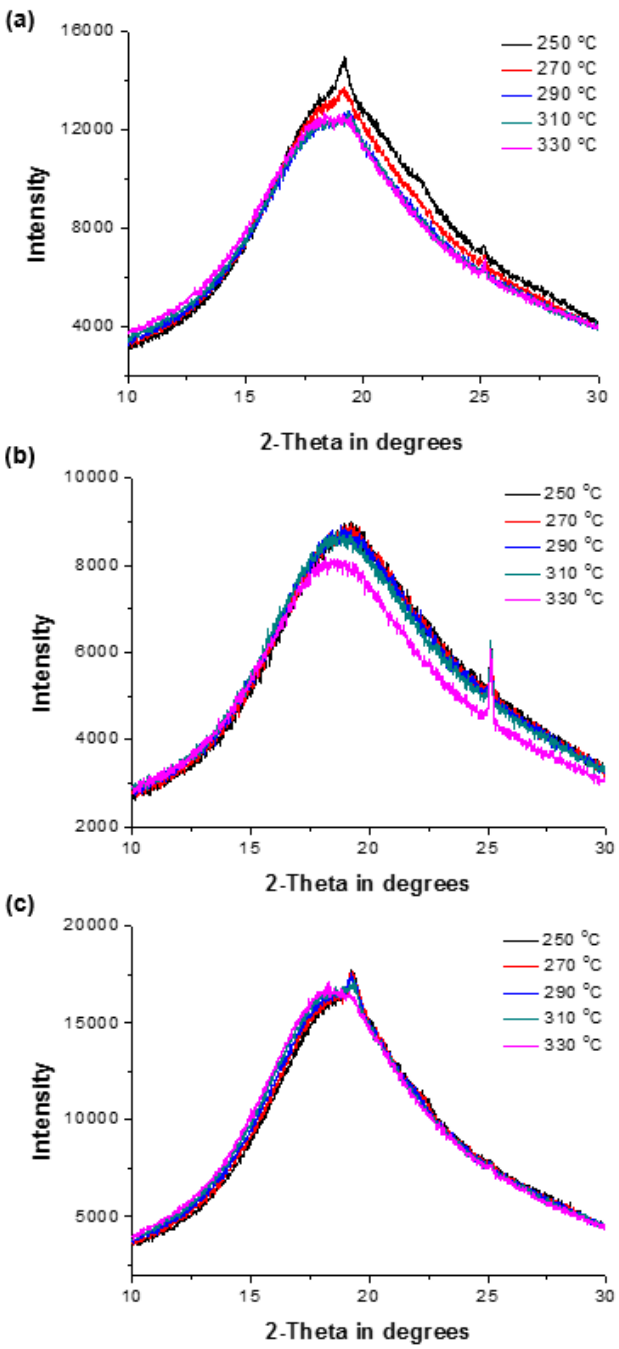

Figure 4-9. WAXS patterns of (a) NR 3/18, (b) NR 5/18 and (c) NR 5/15

Polymer	Temperature	2θ	d-spacing (Å)	FWHM
NR 3/18	250 ºC	19.87	4.47	8.67
	270 ºC	19.82	4.48	8.58
	290 ºC	19.85	4.47	8.73
	310 ºC	19.84	4.47	8.93
	330 ºC	19.82	4.48	9.64
NR 5/18	250 ºC	19.22	4.61	8.11
	270 ºC	19.00	4.67	7.96
	290 ºC	19.00	4.67	7.03
	310 ºC	18.88	4.70	6.82
	330 ºC	18.15	4.89	7.05
NR 5/15	250 ºC	19.25	4.61	12.18
	270 ºC	19.19	4.62	12.45
	290 ºC	19.37	4.58	12.51
	310 ºC	19.35	4.58	12.63
	330 ºC	18.33	4.84	12.45

Table 4-5. WAXS data based on HBA-NHA-resorcinol-TPA

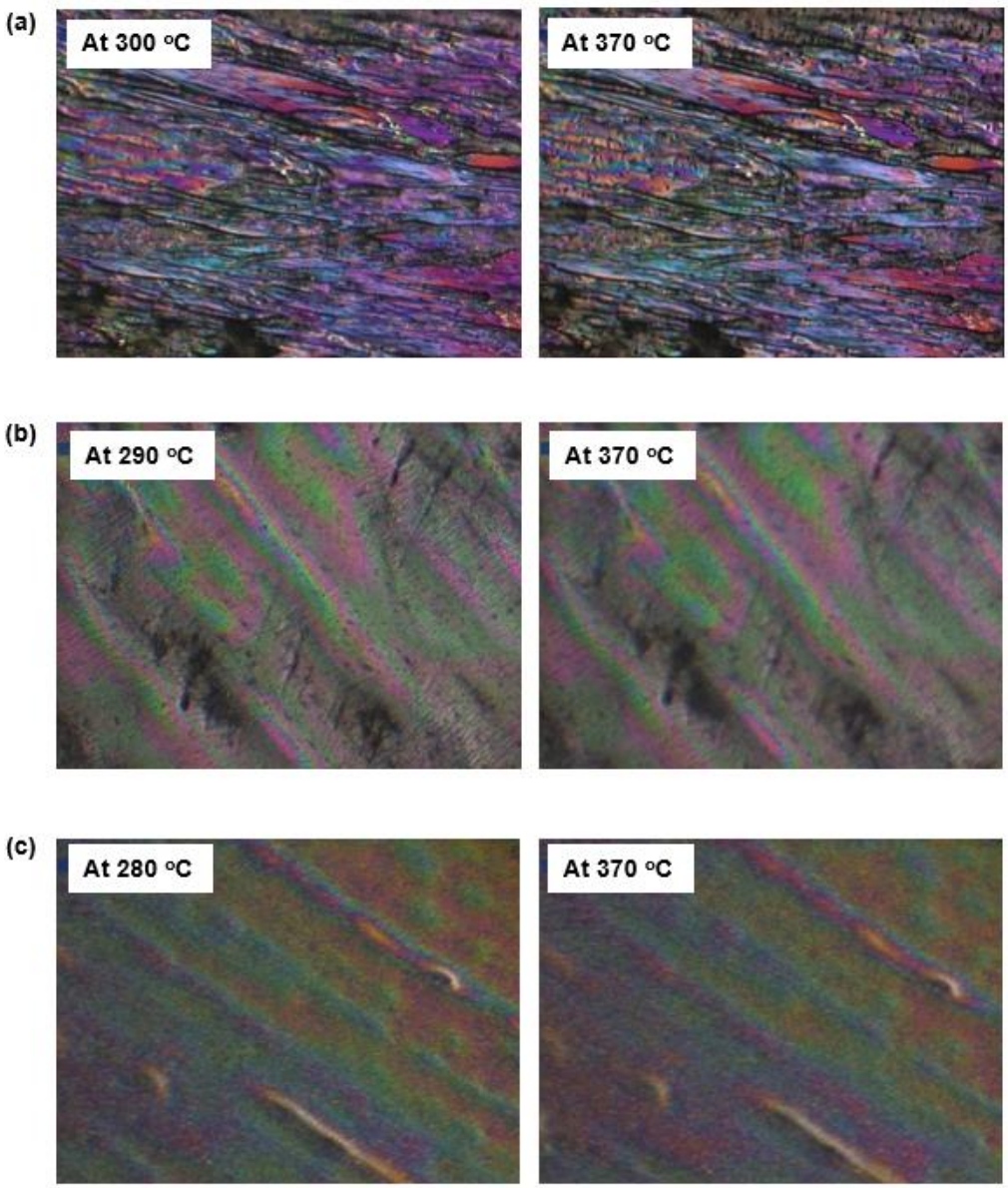

Figure 4-10. Polarizing optical photograph of (a) Resorcinol 10, (b) Resorcinol 15 and (c) Resorcinol 20 (× 5)

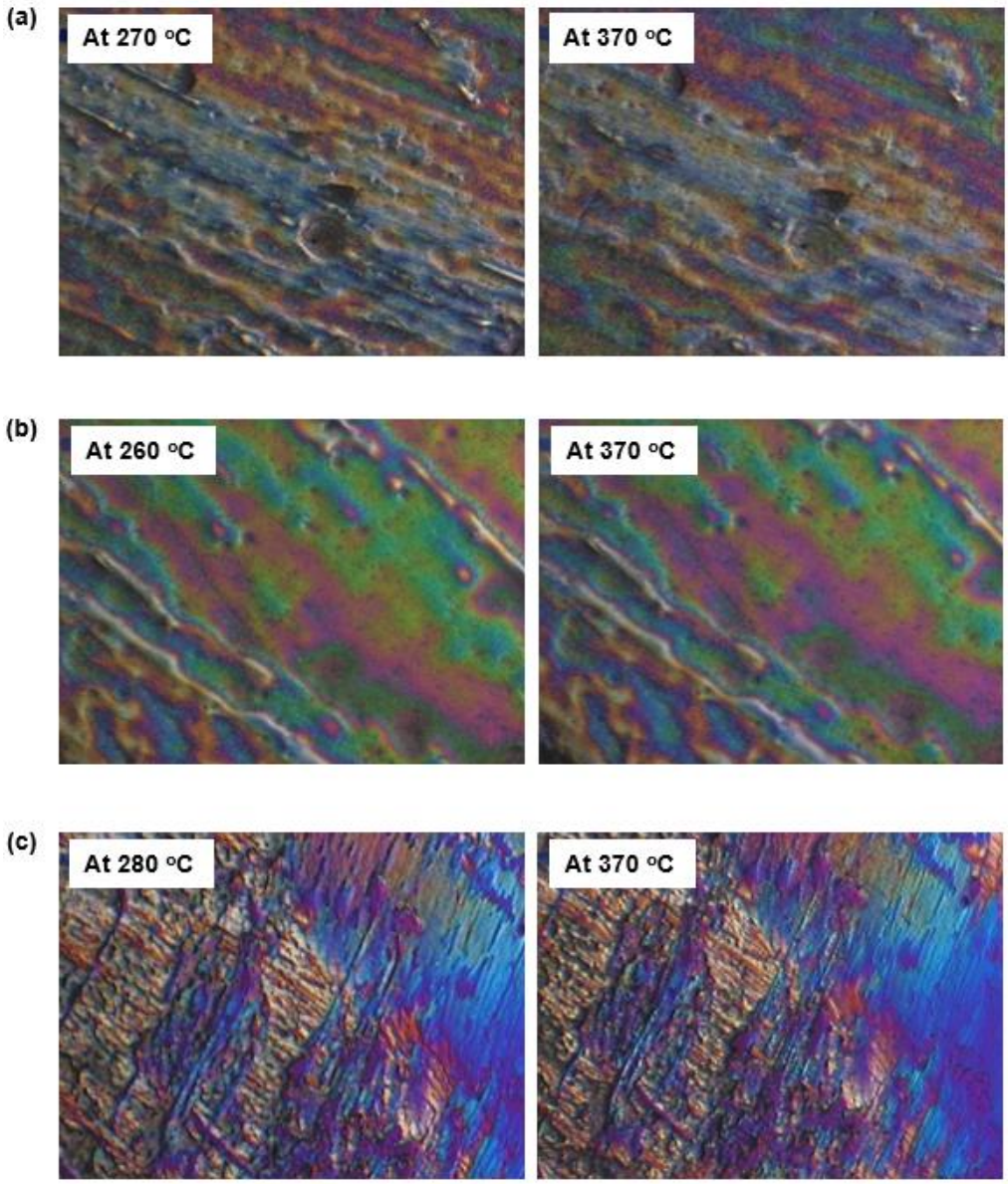

Figure 4-11. Polarizing optical photograph of (a) NR 3/18, (b) NR 5/18 and (c) NR 5/15 (× 5)

In particular, the melting point of Resorcinol 20 was similar to that of commercially available Vectra A, which is about 280 ^{o}C, so that the mechanical properties of the two polymers were compared. Figure 4-12 shows the mechanical properties of Resorcinol 20 and Vectra A. The condensation polymerization, the last step in the polymerization of resorcinol, was conducted with reducing the pressure less than 1 torr using a vacuum oil pump. Three samples were prepared with different polymerization times of 30, 60 and 90 min, respectively. Generally, tensile stress, tensile strain and Young's modulus were enhanced with increasing polymerization time. Sample 90 had tensile stress of 83 MPa, tensile strain of 16.2 % and Young's modulus of 711 MPa, which were 71.5 %, 66.6 % and 93.5 % values of Vectra A, respectively. Although not as excellent as Vectra A, this study shows the potential to replace Vectra A considering the cost of monomers involved in polymerization.

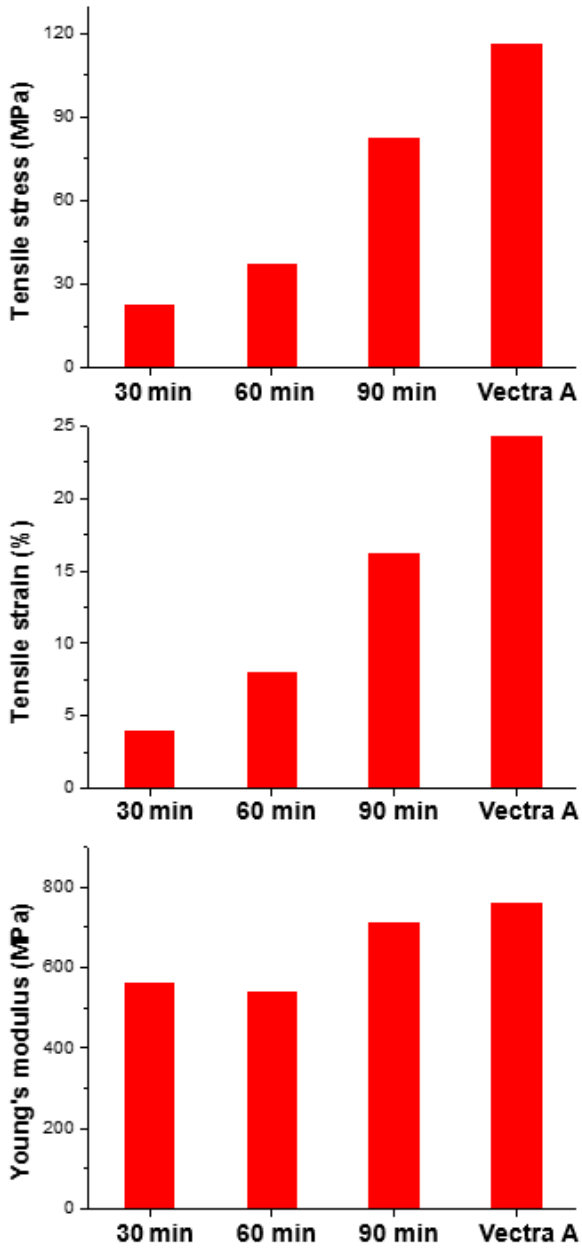

Figure 4-12. Mechanical properties of Resorcinol 20

4.4. Conclusion

HBA-BP-resorcinol-TPA and HBA-HNA-resorcinol-TPA-based TLCPs were polymerized in bulk phase. After activation of the hydroxyl groups of each monomer by acetylation process, oligomerization and polymerization step were conducted resulting TLCPs with excellent properties. Polymers except for Resorcinol 10 and Resorcinol 15 had a limitation in confirming the transition temperature by using DSC. Therefore, the melting point apparatus was used to replace DSC analysis. The thermal stability of polymers was evaluated by TGA and it was confirmed that all of the polymers were stable above 400 ^{o}C. WAXS and polarization microscope were used to determine whether the polymers exhibited liquid crystal behaviors. Among the polymers of various compositions, Resorcinol 20 was evaluated for mechanical properties and the potential of replacing Vectra A, a commercially available TLCP, was confirmed.

4.5. References

[1] M. Jaffe, *Journal of Statistical Physics* **1991**, *62*, 985.

[2] K. C. Yung, H. Liem, H. Choy, T. M. Yue, *Journal of Applied Polymer Science* **2010**, *116*, 2348.

[3] M. Zhou, V. Frydman, L. Frydman, *J. Phys. Chem.* **1996**, *100*, 19280.

[4] T. I. Bair, P. W. Morgan, F. L. Killian, *Macromolecules* **1977**, *10*, 1396.

[5] H. R. Kricheldorf, G. Schwarz, *Makromol. Chem.* **1983**, *4*, 475.

[6] M. Koike, C.-C Yen, L. Yuqing, H. Tsuchiya, M. Tokita, S. Kawauchi, H. Takezoe, J. Watanabe, *Macromolecules* **2007**, *40*, 2524.

[7] D. J. Williams, *Advances in Polymer Technology* **1990**, *10*, 173.

[8] P. Tang, J. A. Reimer, M. M. Denn, *Macromolecules* **1993**, *26*, 4269.

[9] G. Costa, D. Meli, Y. Song, A. Turturro, B. Valenti, M. Castellano, L. Falqui, *Polymer* **2001**, *42*, 8035.

[10] G. D. Choi, S. H. Kim, W. H. Jo, M. S. Rhim, *Journal of Applied Polymer Science* **1995**, *55*, 561.

[11] T.-T. Hsieh, C. Tiu, K.-H. Hsieh, G. P. Simon, *Korea-Australia Rheology Journal* **1999**, *11*, 255.

[12] W. J. Jackson, *Polymer International* **1980**, *12*, 154.

[13] N. Khan, Z. Bashir, D. M. Price, *Journal of Applied Polymer Science* **1995**, *58*, 1509.

[14] D. Dong, S. Jiang, Y. Ni, B. Jiang, *European Polymer Journal* **2001**, *37*, 611.

[15] Z. Yerlikaya, S. Aksoy, E. Bayramli, *Journal of Polymer Science* **2002**, *85*, 2580.

[16] Z. Yerlikaya, S. Aksoy, E. Bayramli, *Journal of Polymer Science* **2003**, *90*, 3260.

[17] A. B. Padias, H. K. Hall, *Polymers* **2011**, *3*, 833.

[18] I. Nitta, K. Asai, H. Harada, US Patent 5,399,656: 1995

[19] U. Shukla, K. V. Rao, A. K. Rakshit, *Journal of Applied Polymer Science* **2003**, *88*, 153.

[20] L.-L. Lin, J.-L. Hong, *Polymers* **2000**, *41*, 2419.

국문 요약

인쇄회로기판은 절연판 위에 전자 부품 및 반도체를 연결해주고 지지해주는 역할을 한다. 전자 기기 제품의 소형화에 따른 다층 기판의 사용이 요구되기에 절연성과 내열성 그리고 기계적 강도가 우수한 재료 물질의 연구가 진행 중에 있다. 가장 상용화되어 있는 열경화 소재인 에폭시는 가격이 저렴하고 분자 구조 조절이 용이하며 절연성이 높다. 또한 기계적 물성이 우수한 무기물질과의 복합 소재 개발이 용이하지만 경화 과정 메커니즘에 의하여 열경화 과정에서 하이드록실기가 생성되는데 이는 전기 절연성의 평가 척도인 유전 정접 값에 부정적인 효과를 나타낸다. 벤조옥사진은 단순 열 조건에 의해 가교화 되는 열경화 소재로, 아민 단량체와 하이드록실 단량체 그리고 파라포름알데히드의 존재 하에 벌크상이나 용액상에서 비교적 짧은 시간에 합성 된다. 이러한 벤조옥사진은 열적 안정성, 기계적 물성 그리고 절기 절연 특성이 우수하다. 열경화 과정에서 생성되는 하이드록실기는 분자 간, 분자 내 수소 결합으로 단단히 고정 되어 있기 때문에 전기 절연 물질로 알려져 있다.

벤조옥사진은 열경화 과정에서 생성되는 하이드록실기가 수소 결합으로 묶여 있기 때문에 기판의 제작에 사용되는 동박과

의 접합력이 제한된다. 2 단원에서는 벤조옥사진과 에폭시 블렌드 조성에 실리카 나노입자를 분산 시켜 하이브리드 필름 개발을 연구한 결과를 나타낸다. 상용화 되어 있는 모노 벤조옥사진인 BA-a 기반의 하이브리드 필름을 제작하였고, 에폭시 대비 벤조옥사진의 함량 증가에 따라 유전 정접 값이 감소 되는 것을 확인하였다. 하지만 모노 벤조옥사진 자체의 취성에 의해 기계적 강도에 한계가 있어 선형 폴리벤조옥사진을 도입하였다. 선형 폴리벤조옥사진과 에폭시 블렌드 조성에 실리카 나노입자를 분산함에 따라 유전 정접 값이 감소 되었고 동박에 접합력이 우수한 것으로 확인하였다. 다음 연구에서는 시아노 기를 벤조옥사진에 도입하여 절연성이 우수한 필름 개발을 하였다. 3 단원에서는 시아노기를 포함하는 모노 벤조옥사진과 에폭시 블렌드 조성에 실리카 나노입자를 분산시키는 과정을 통해 필름을 제작하여 유전 정접 값을 평가하였다. 시아노기는 열경화 과정을 통해 트라이진 고리를 형성하는데 이러한 구조 때문에 전기 음성도가 희석되어 보다 강화된 절연성을 나타내게 된다. 연구 결과 상용화 되어 있는 벤조옥사진인 BA-a 기반의 필름 비교하여 더욱 감소 된 유전 정접 값을 나타내었다. 하지만 시아노-벤조옥사진 역시 BA-a 처럼 단량체 구조이기에 취성을 나타내어 필름의 물성이 보강된 연구가 필요하다.

액정이란 액체와 결정의 중간 상태에 있는 물질로 액체 상태를 유지하며 배열이 규칙적인 결정 상태를 나타낸다. 액정은 열방성과 유방성으로 분류 되는데 이번에 연구 된 것은 열방성 액정 고분자로 융점 이상에서 등방성 액체로 변하지 않고 비등방성 용

융 상태를 유지하는 특징을 나타낸다. 이러한 액정 고분자는 강철의 5 배 탄성율과 강도를 가지는 고성능 섬유이기에 그 활용도가 높다. 대표적으로 알려진 액정고분자는 케블라와 에코놀로 방탄복이나 특수한 환경에 노출되는 제품에 사용되는데 융점이 매우 높아 활용에 제한이 있다. 이를 극복하고자 벡트라 제품이 상용화 개발되었고 융점이 280 도로 가공성이 우수하다. 4 단원에서는 융점 조절이 용이하고 상업적으로 활용이 가능한 열방성 액정 폴리에스터 중합 연구를 평가하였다. 벡트라에 첨가 된 단량체인 HNA 가 고가이기에 이를 대체하고자 레소시놀 단량체를 도입하였고 축합 중합 결과 얻어진 중합체의 기계적 물성이 벡트라 비교하여 비교적 우수하였기에 상용화 될 수 있는 가능성을 확인하였다.

주요어 : 벤조옥사진, 에폭시, 실리카, 하이브리드 필름, 유전정접, 액정 고분자, 열방성 액정 폴리에스터, 융점

학 번 : 2010-23194